Materials Today Chemistry 12 (2019) 96–120

Contents lists available at ScienceDirect

Materials Today Chemistry

journal homepage: www.journals.elsevier.com/materials-today-chemistry/

Speeding up the unique assets of atomic layer deposition

D. Muñoz-Rojas [a, *], T. Maindron [b], A. Esteve [c], F. Piallat [d], J.C.S. Kools [e], J.-M. Decams [f]

[a] Univ. Grenoble Alpes, CNRS, Grenoble INP, LMGP, F-38000 Grenoble, France
[b] Université Grenoble-Alpes, CEA, LETI, MINATEC Campus, 17 Rue des Martyrs, F-38054 Grenoble, France
[c] University of Toulouse, LAAS-CNRS, 7 Avenue du Colonel Roche, 31031 Toulouse, France
[d] KOBUS, 611 Rue Aristide Bergès, 38330 Montbonnot Saint Martin, France
[e] Encapsulix SAS, 481 Chemin Des Vignes, 13109 Simiane-Collongue, France
[f] Annealsys, 139 Rue des Walkyries, 34000 Montpellier, France

ARTICLE INFO

Article history:
Received 20 July 2018
Received in revised form
6 November 2018
Accepted 30 November 2018
Available online 28 January 2019

Keywords:
High-throughput
Batch ALD
Spatial ALD
Modeling
Encapsulation
Process engineering

ABSTRACT

Atomic layer deposition (ALD) has been traditionally regarded as an extremely powerful but slow thin-film deposition technique. The (perceived) limitation in terms of deposition rate has resulted in a slow penetration of the technology into mass manufacturing beyond established applications in the semiconductor industry until recently. At present, several developments have resulted in a significant increase in the use of ALD in a number of mass manufacturing applications. On the one hand, there is an increasing demand from the device makers side to incorporate nanotechnology in their products that relies on the unique advantages of ALD. On the other hand, a number of technical improvements have been implemented in the ALD method allowing it to be much faster. In this article, we provide an overview of different high-throughput (HT) ALD approaches, putting them in perspective with other common HT deposition techniques already used in the industry. As an example, the use of HT ALD for the encapsulation of organic light-emitting diode is discussed.

1. Introduction

In the last years, nanoscience and nanotechnology have represented a revolution in the way we study, understand, and exploit materials through the synthesis and fabrication of advanced devices. But nanomaterials themselves and their utilization are far more ancient. The typical example is the Lycurgus cup made in Roman times, where the presence of nanoparticles confers the attractive optical properties of the cup. Another example is the colored glasses in stained windows in thousands of medieval churches across Europe, where nanomaterials play again a key role in the final color [1]. The issue is that users of nanomaterials in past times had no way of knowing that they were dealing with nano-objects. Indeed, what drove the outcome of nanoscience was the development of powerful characterization tools that allowed us to probe the nanoworld, such as electron microscopy and scanning probe microscopy, among others. With these powerful tools, one could start walking the spacious bottom [2] and understanding the new phenomena appearing as a result of having materials at the nanoscale. The passage from nanoscience to nanotechnology involved yet another development in equipment and processing technologies. The fancy early example of writing with atoms using an scanning tunneling microscope (STM) [3] has been followed by more sophisticated and useful techniques [4].

A clear example of these novel processing methods allowing to control matter at the nanoscale is the atomic layer deposition (ALD) technique. ALD is a chemical vapor deposition (CVD) technique, i.e. where precursors in the gas phase react with a surface to form a film. In conventional CVD, volatile metal precursors are sent into the deposition chamber along with the reactant precursors and the reaction yielding the formation of a thin film on the substrate is activated by heat, plasma, or any other means to bring the required energy for the reaction [5]. In CVD, gas diffusion and fluid dynamics play a key role in the quality and homogeneity of the films deposited, and the reaction can be controlled either by diffusion of precursors or by kinetics. While CVD is an excellent technique used by industry for many years now and capable of yielding high-quality films from tens to thousands of nanometers thick, it has various limitations. The activation of the reaction near the surface and the role of diffusion and fluid dynamics inherent to CVD are at the origin of such limitations. Thus, it is not trivial to (i) deposit homogeneous thin films over large areas such as required for large

* Corresponding author.
E-mail address: david.munoz-rojas@grenoble-inp.fr (D. Muñoz-Rojas).

https://doi.org/10.1016/j.mtchem.2018.11.013
2468-5194/

displays; and (ii) have highly conformal films over high-aspect-ratio features or complex porous substrates. These difficulties inherent to CVD can be controlled, and for instance, the glass industry uses different CVD approaches to coat large-area flat glass substrates and even complex shapes such as bottles. But the processes used only work for molecular precursors (i.e. Si and Sn precursors). In addition to homogeneity, conformality, and thickness control, when compared with CVD, ALD offers a wide panoply of materials that can be deposited on large-area and complex substrates.

The need for homogenous films for large-area displays and of highly conformal coatings for the microelectronics industry drove the invention and development of ALD. In ALD, patented by Suntola and Antson in 1977 [6] and also developed previously by Russian researchers [7,8], volatile and thermally stable precursors are injected sequentially, as illustrated in Fig. 1a. First, the organometallic precursor is injected, and enough time is given for it to react (hydrolysis/condensation) with active sites on the surface. The reaction involves the breakage and formation of bonds, yielding a chemisorbed layer on the surface of the substrate. As opposed to what happens in CVD, the precursor should not decompose thermally above the substrate. Indeed, when comparing the required properties of CVD vs. ALD precursors, most of them are shared, but in the case of ALD precursors, they must be highly reactive yet thermally stable, as stated above [9]. Once the precursor has reacted with all the active sites on the surface, excess precursor and byproducts are purged, and the second precursor is injected. After reaction with the first monolayer, excess precursor and byproducts are purged again before proceeding with the same steps in a cyclic manner (Fig. 1a). Thus, ALD is characterized by being a surface-limited, self-terminated method where fluid dynamics plays a minor role, diffusion being the most important parameter allowing

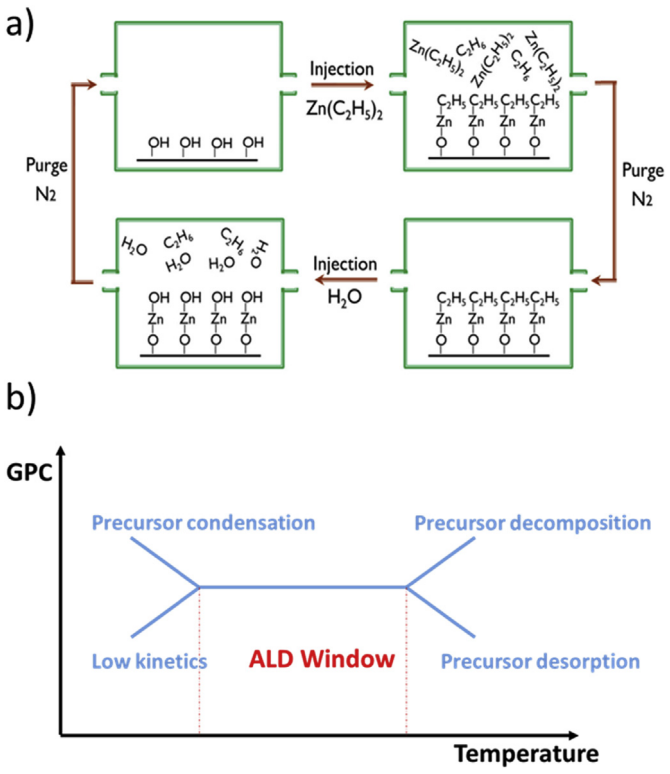

Fig. 1. (a) Scheme of the atomic layer deposition (ALD) process for the deposition of ZnO, showing the alternative steps: a first precursor (DEZ, diethylzinc) is injected and a purge occurs followed by the injection of the second precursor (water) and so on. (b) Scheme of the typical growth per cycle (GPC) as a function of temperature in ALD.

precursor molecules to reach every part of the surface to be coated. As a result, very homogeneous films with a precise control over thickness, down to the monolayer thickness, can be achieved. This includes films over large areas or highly conformal films on high-aspect-ratio features or complex substrates. In addition, because of the highly reactive nature of ALD precursors, high-quality films can be obtained at lower temperatures than CVD. ALD reactions are characterized by a temperature range (called ALD window) in which growth per cycle (GPC) stays constant. Out of the ALD window, the GPC can be lower due to low kinetics (low T) or desorption during the purge step (high T) or higher due to condensation of precursor (low T) or thermal decomposition of the precursors such as in CVD (high T), as shown in Fig. 1b).

It is obvious that a technique with such qualities is very attractive for nanoscience and nanotechnology research, where surfaces and interfaces need to be engineered at the nanoscale. As a result, the application of ALD in research and development has experienced a boom in the last years and is now a well-stablished technique at the laboratory scale, with a large choice of suppliers of research ALD equipment, which keeps increasing [10]. The number of papers in which ALD is involved also increases, and so do the applications targeted, which include photovoltaics, fuel cells, environmental applications, anticorrosion, passivation, encapsulation, or sensing. ALD has been widely reviewed in the past, including specific applications of ALD [11–19]. We refer the reader to the references for more details. Concerning the industrial application of ALD, one could expect a similar trend to what has been observed at the laboratory scale. Unfortunately, apart from some applications on very high added value products in the semiconductor and related industries, this has not been the case. The reason for this slow adaptation is the low deposition rate of ALD, especially at low temperature, in general around 0.15 nm/s, and thus much slower than CVD or physical vapor deposition (PVD) techniques (see Table 1). The cyclic nature of ALD, with long injection/saturation pulses and even longer purge steps, is the reason for the low deposition rate. It is even worse for large substrates, where the volume of the ALD reactor does increase and so does the time needed for pulsing and purging. In addition, the fact that most ALD processes take place under vacuum (to accelerate the purge and because of the traditional utilization of ALD for microelectronics) implies another drawback for industrial implementation because of the high cost involved when scaling up vacuum equipment.

The main industrial applications of ALD are still the original ones for which the technique was developed, i.e. microelectronics and large-area displays (historically thin-film electroluminescent display and more recently organic light-emitting diodes [OLEDs]). Even more, microelectronics and the need to reduce further the fabrication scale and even to go to 3D architectures is still a strong driver for the development of ALD and for pushing the penetration of ALD into production [20]. As done in research laboratories, ALD could be applied industrially in many more applications, but for that to happen, high deposition rates, i.e. high-throughput (HT), are needed, while vacuum-free processing is desirable, because most applications do not share the added value of microelectronic products. In microelectronics, the finished product has a high value per m^2 (e.g. more than 10 k€ for a completed 300 mm wafer), while for example in photovoltaics, an application for which ALD is largely applied in research, the value of finished products is nominally/ideally less than 100 € per m^2. Of course, the required uniformity, repeatability, and number of process steps are higher in microelectronics, altogether leading to higher cost. Nevertheless, the available budget per process step is orders of magnitude lower in these non-microelectronic applications. Thus, HT ALD would become an enabling innovation for many applications because while the technical performance may

Table 1
Comparison between ALD, CVD, and PVD deposition techniques.

Property	ALD (cross-flow)	PE-CVD	PVD
Growth mode	2D	Nucleation	Nucleation
Thickness control	Digital control (given by the number of cycles, depending on precursors/materials)	Good from tenths of nm	Not suited for nanometer-scale thickness
Film conformality	High	Moderate	Low
Film quality	Pinhole-free, low stress	Pinholes moderate, stress moderate	High pinhole density, high stress
Typical deposition speed	2.5×10^{-3} nm/s (standard cross-flow R&D reactor)	0.1–10 nm/s	0.1–10 nm/s

ALD, atomic layer deposition; CVD, chemical vapor deposition; PE, plasma enhanced; PVD, physical vapor deposition.

have been proven a long time ago, standard ALD is just economically unfeasible. The same applies to other techniques related to nanoscience and nanotechnology, the development of which should contribute to the outcome of what has been called nanomanufacturing [21,22].

Because ALD offers unique qualities that no other technique can offer, it is desirable that any device/technology/product development involving ALD should be scalable and implemented with HT ALD. In the last years, there has been a huge progress toward faster ALD processes. Different approaches have been tackled, including batch ALD, spatial ALD (SALD), process engineering, and reactor optimization. We present here these HT ALD approaches to show that rather than the *Awfully Long Deposition* technique that ALD used to be considered, it can already be regarded as a HT technique, with different approaches proving so. The description of the different HT ALD approaches is preceded by a section in which the different performance metrics allowing a fair comparison between the different HT ALD approaches and with other deposition techniques is given. As it will be shown below, in the HT ALD approaches presented here, fluid dynamics are back in the game and must be considered when designing reactors and for process engineering. A section dealing with modeling of HT ALD is thus included. We will then provide a case study in which we will discuss the use of HT ALD for thin-film encapsulation of atmosphere-sensitive devices such as OLEDs. We will finish by giving a perspective on the challenges that still lay ahead for HT ALD. This review does not intend to be exhaustive regarding the different HP ALD systems available in the market. Rather, the authors have focused on the approaches with which they are more familiar as a way of illustrating the different possibilities. We hope this review will provide a wide overview of the HT ALD landscape, helping researchers and companies to make the right choices when moving into the (HT) ALD field.

2. Performance metrics

Owing to the different particularities and specifications of the different existing approaches to HT ALD, it is not always simple to make comparisons between them and with other deposition techniques. Several metrics can be used to quantify the speed of a thin-film deposition process so that different processes can be readily compared. These are detailed below:

Deposition rate (in nm/s) describes the speed at which a coating grows on the substrate and thus provides a basic characterization of the process.

Takt time (in s) provides the time in between different substrates for an inline process. Alternatively, *throughput* (in substrates per hour) provides the number of substrates processed per time unit. These quantities also include information on the thickness of the coating, the number of substrates processed in parallel, and the overhead time for substrate heating, cooling, pump down, venting, transfer, etc. A slightly modified metric is *area throughput* (m^2/h) which normalizes for the size of the substrate and is specifically used for large area applications.

Cost of ownership (in \$, € or ¥ per m^2 of product) will take into account several economic factors. The total cost per substrate processed is calculated using the different cost contributions such as the cost of equipment (both initial investment and maintenance cost), cost of consumables, facilities, labor, cost of capital and administrative overhead, divided by the number of substrates processed successfully. In addition to the raw throughput, factors such as scrapping of substrates (i.e. destruction of product being progressed by imperfect processing), uptime (percentage of the time that the tool is available for production), utilization (i.e. percentage of the time that the tool is available and actually being used to produce sellable product) are also parts of the economical requirements. Depending on the type of utilization, the relative importance of these factors differs. For example, for a batch process near the end of the production process of a high-value product, a single tool failure may result in a revenue loss that can be comparable to the cost of the tool. The evaluation of cost of ownership (or even throughput/takt time) must be done on a case by case basis and is therefore beyond the scope of this review. Instead, we will focus on basic metrics such as deposition rate.

In the case of ALD, two parameters are of foremost importance when evaluating deposition rate: GPC and the cycle time. GPC under fully saturated ALD conditions is determined by chemistry and temperature (see Fig. 1b). In most cases, it is not possible to vary these parameters, and therefore, the GPC is to be considered a constant. Nevertheless, some precursor chemistries provide a path to substantially increase the GPC for a given temperature and material system. For example, in the case of low-temperature deposition of Al_2O_3, it has been found that the GPC in PE ALD is around 1.5–2.0 Å/cycle, while it is in the range 0.6–1 Å/cycle for thermal ALD. The cycle time is the sum of purge times and pulse times during one single ALD cycle. Pulse times are determined by the requirement to absorb a sufficient number of precursor molecules to reach substrate saturation. For many reactive chemistries, pulse times can be very short (tens of milliseconds), but for less reactive chemistries or low vapor pressure precursors, it is not necessarily the case. Purge times are determined by the time to clear the reactants from the reactor. Traditionally, purge times have been quite long (seconds), especially at low deposition temperature and thus the determining factor for the cycle time and thus the deposition rate.

3. ALD approaches to HT

As stated above, there are four main approaches that have been developed and that allow performing ALD at high deposition rates: Batch ALD, SALD, process engineering, and reactor optimization. In the following sections, a description of these different approaches and their current industrial utilization is provided.

3.1. Batch ALD

The simplest and thus more mature approach toward HT ALD is the use of batch reactors in which more than one substrate can be coated at the same time. Batch ALD has been used from many years

now in production, mainly in microelectronics (were Si wafers are the usual substrate), and the different manufacturers of industrial ALD equipment offer bath tools adapted to different applications. In batch ALD, because the reactors are bigger, the ALD cycles have to be longer to ensure the complete formation of monolayers on the substrates and also ensure an efficient purge, the limiting factor being the diffusion of precursors between the wafers. For this same reason, lower operation pressures are usually necessary for batch ALD to have efficient convective and diffusive purging. Despite both longer cycles and longer overhead times, batch ALD yields a higher number of samples per hour, thanks to the higher number of samples coated simultaneously. For instance, Granneman et al. compared the deposition of 10 nm thick HfO_2 films using batch and single wafer systems. The results showed, respectively, a throughput of 16 and 7 wafers/h [23].

Also, owing to the high reactivity of ALD precursors and the fact that in most cases the reactor temperature is the same as the sample temperature (i.e. the whole deposition chamber is heated at a certain temperature), deposition takes place on the walls of the reactor, thus causing a waste in precursor which contributes to the final price per substrate. In batch ALD, because the ratio between the sample surface and reactor surface is higher, a more efficient use or precursors is obtained (30% reported for Al_2O_3) [24]. Conversely, the higher volumes involved in batch ALD can cause a narrowing of the ALD window. In the low temperatures, precursor condensation can be an issue on the first wafers exposed to the precursor. In the high temperature range, lower maximum temperatures with respect to single wafer ALD are attainable as the longer cycles can yield thermal decomposition of the precursors while saturation of all the substrates is taking place. In the same manner, the exposure to high temperatures during longer times can cause precursor desorption prior reaction with the second reactant. This, in addition, can affect cycle time because the possibility of using higher temperatures would induce a slight reduction in purge time because of a higher gas velocity and diffusion coefficient.

But overall, the advantages of batch ALD in terms of throughput overcome the drawbacks that it presents. In a study from 2014, Dingemans et al. presented the merits of batch ALD processing by evaluating different materials and applications [24]. As a result, a series of merits of batch ALD, in addition to the intrinsic characteristics of ALD, were listed:

- Reactors with capacities of up to 170 wafers, with cycle times of only 28 s (i.e. cycles of 0.16 s per wafer).
- Low cost thanks to small system footprint, efficient use of precursor, and competitive pricing.
- Sequential batch processing is possible
- Large freedom in cycle time optimization, not affected by hardware limitations (e.g. switching speed of valves)

Batch ALD can be optimized, thanks to reactor design using simulations. Indeed, the concentration of the precursors in different locations of the reactor after a certain time following the injection of precursor depends on how the precursors are injected and on the reactor design. Simulations of a vertical batch reactor with one single precursor inlet at the top and another one with a multiple precursor inlet have been performed, showing a higher homogeneity in terms of precursor distribution with time for the multiple inlet reactor (see Fig. 2).

Although batch ALD is used in the microelectronics industry, the throughput obtained would still be too low for other applications, such as the passivation of silicon solar cells with Al_2O_3 layers. To increase the throughput and make batch ALD more competitive with respect to PE-CVD, side improvements are investigated. Beneq, for example, has explored the use of a fully automated system for wafer handling, together with sample preheating [25]. Standard batch ALD tools from Picosun are, on the other hand, used to deposit protective anticorrosion layers on commemorative coins and to provide color to jewelry components [26].

3.2. Spatial ALD

As it has been explained in the introduction, the key characteristic of ALD with respect to classical CVD is the sequential exposition of the substrate to the different precursors to have surface-limited and self-terminated reactions. This separation was traditionally made by separating precursors in time in a sequence of injection/purge steps. Another possibility is to separate the precursors in different locations of the reactor, i.e. spatial separation. In SALD, as it is most commonly known, precursors are continuously injected in specific locations and fashions, which depend on the system design, and are kept apart by regions containing an inert gas, typically N_2. It is interesting to note that SALD was already described in Suntola and Antson's first ALD patent in the 1970's [6]. Even more, the first apparatuses proposed in the patent are spatial, while more standard temporal ALD apparatuses are presented afterward. In this patent, ALD was mostly inspired by sputtering and molecular beam epitaxy (MBE), and thus the precursors proposed were single elements such as Zn and S to deposit ZnS or Sn and O_2 for SnO_2. Some years later, in 1983, Suntola showed in a second patent that an effective precursor separation can be achieved even at atmospheric pressure, without the need of unrealistically high gas flows, if ingenious systems are conceived. This led to the development of atmospheric pressure SALD (AP-SALD) [27]. In this patent, ALD is already closer to CVD as metal-organic precursors are considered. Despite the early presentation of SALD, it was not until 2008 that the first publications and patents came out, mainly by Kodak and TNO. In the first SALD article by Levy et al., an open-air SALD approach was presented and used to fabricate ZnO-based thin film transistors (TFT) [28]. In their report, both the Al_2O_3 dielectric layer and the ZnO gate oxide were deposited at atmospheric pressure, in the open air, obtaining working devices with good properties. Kodak's approach is based on a manifold injection head where the gas flows containing the different precursors are separated in parallel channels, alternated with channels containing only N_2. By placing the substrate close enough to the head (typically on the order of 50–200 μm, which can be adjusted mechanically or using a gas bearing system), an efficient separation of precursors can be achieved. Owing to the small gap used between the head and the substrate to prevent precursor crosstalk, this approach is known as 'close-proximity SALD' (see Fig. 3).

Kodak's systems were used and further optimized by Prof. Driscoll's group at the University of Cambridge for the deposition of components for new generation solar cells [29]. The high deposition rate inherent to SALD has allowed the fundamental study of device physics by using doped oxides or extra-thin interfacial layers [30–38]. TNO was also among the first to patent and report SALD systems [39]. In 2010, this group also showed that SALD could be used to deposit a very efficient Al_2O_3 passivation layers on crystalline Si solar cells, reducing charge recombination [40]. The high passivation efficiency obtained together with the high deposition rate and atmospheric processing resulted in the creation of SoLayTec, a spin-off company that commercializes both large-scale and pilot plant tools for the passivation of Si solar cells. Levitech is another company that also commercializes a similar tool for the same application. These tools have demonstrated that SALD can provide very HTs, of up to 6000 wafers/h (with deposition rates above 1 nm/s). At the research level, reports from different groups

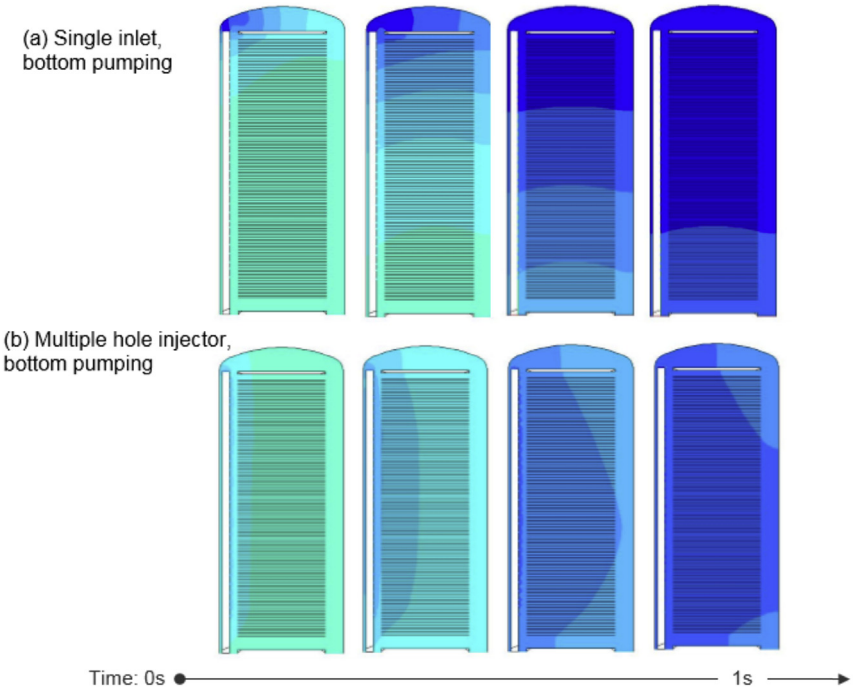

Fig. 2. Contour plots of precursor ($TiCl_4$) partial pressure at different times after precursor injection in two similar batch reactors. (a) Single inlet reactor. (b) Multiple inlet reactor. Reprinted from Ref. [24] with permission.

have shown that SALD can be up to two orders of magnitude faster than temporal ALD [41].

In addition to high rates, the spatial separation of precursors has proven to be a very flexible concept, allowing the design of many different types of reactors. A review by Poodt et al. (2012) described some of the early reactors, many of them using the close-proximity approach [42]. Since then, other systems were reported. Some of the reactors are designed to be compatible with roll-to-roll (R2R) mode [43–52], while the possibility to work in the open air facilitates *in situ* characterization [49]. Also, a recent report presented a comparison of the deposition of ZnO coatings with different SALD systems and conventional ALD [53]. It is shown that intrinsic and doped ZnO films can be deposited with tuned optical and electronic properties, which resulted in devices with record efficiencies in some cases, confirming the high quality of SALD coatings. Deposition rates vary a bit depending on the reactor and conditions used, being up to 2 nm/s, as compared with 0.13–0.18 nm/s for a conventional ALD system. In terms of GPC, similar values are obtained for both SALD and ALD, as expected since the chemistry is the same. The concept of cycle in SALD can be confusing because the different SALD systems differ in mode of operation and design, which results in different types of SALD cycle, with different equivalences between SALD cycles and conventional ALD cycles. Therefore, comparisons should be done in terms of nm/s or wafers/h to avoid confusion.

As shown above, the initial applications of SALD focused on microelectronics and photovoltaics. The application of SALD to the fabrication of TFT devices has been pursued by Kodak, and their initial publication of 2008 has been followed by the development of area-selective deposition with SALD, which provides design freedom and has allowed to improve the yield and performance of the devices fabricated [54–58]. SALD has also proven very effective for the deposition of components for new generation solar cells. In one of the first examples, TiO_2 blocking layers were deposited by SALD for bulk heterojunction solar cells. The results showed that an amorphous TiO_2 film only 13 nm thick and deposited at 100 °C yields the same performance than an 80 nm thick crystalline TiO_2 film deposited by Spray pyrolysis at 450 °C. As SALD yields films with the same quality as conventional ALD, extremely thin blocking layers can be deposited. And thus, amorphous TiO_2 can be used without contributing much to the series resistance of the device. And because crystallinity is not needed, low deposition

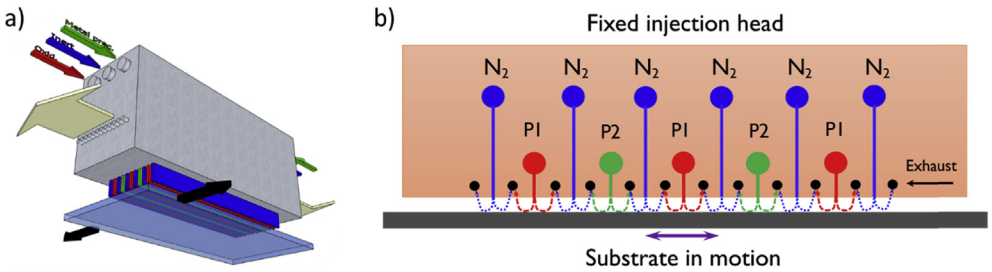

Fig. 3. a) Scheme of a SALD close-proximity head in which the substrate is oscillated below the slots through which the different precursors are continuously injected. (b) Side-view of the head-substrate gap showing the paths of the different flows that take place for the small gap used, which ensure no precursor crosstalk. ALD, atomic layer deposition; SALD, spatial ALD.

temperatures, compatible with plastic substrates (relevant for organic photovoltaics), can be used. The combination of high deposition rate and the possibility of using extremely thin films resulted in two orders of magnitude faster deposition rates, as compared with other low-temperature atmospheric methods reported to deposit TiO_2 blocking layers [37]. In addition, the possibility to use an extremely thin blocking layer contributes to a lower cost since less material is used (which is also highly important in terms of making an efficient use or raw materials, in particular, if they contain critical elements) [59]. The HT offered by SALD was used by Prof. Driscoll's group to perform fundamental studies on the physics of new generation photovoltaic devices [29–36,38,41,60]. The same group also used the possibility of low-temperature processing to deposit ZnO layers as an electron injector in a hybrid perovskite-based LED [61]. More recently, research from the Laboratoire des Matériaux et du Génie Physique (LMGP) has shown the benefits in coupling SALD with transparent electrodes based on metallic nanowire (MNW, mainly Ag and Cu) networks. MNW networks are very promising since they can have higher transparency and conductivity than standard oxide-based transparent electrodes and are also flexible [62,63]. These types of electrodes can be processed at ambient pressure and from solution but need to be coated to increase their chemical, electrical, and thermal stability. The fast deposition rate together with low-temperature and ambient processing makes this SALD very attractive to coat AgNW networks with conformal oxide layers, rendering the electrodes much more stable [62,64,65].

The number of reports involving SALD is showing a steady increase since the first report in 2008, and applications have expanded from the initial studies focusing on TFT and solar cells. To date, SALD has been extensively used for encapsulation, to protect devices, or to fabricate gas diffusion barriers, both in rigid and flexible substrates, including paper, as detailed below [44,48,64,66–73]. Choi et al. have demonstrated Al_2O_3 deposition rates as high as 7 nm/min (0.12 nm/s) at temperatures below 100 °C. The SALD system they have developed is coupled to a glove box and can coat substrates of industrial size (370 × 470 mm^2). They used it to encapsulate OLEDs, which showed little degradation and sustainable emission properties when using a 50 nm thick Al_2O_3 encapsulating layer [71]. The versatility provided by the possibility to perform deposition at ambient pressure with SALD was exploited by Mutee ur Rehman et al. to combine it with the deposition of organic films by spray to obtain hybrid, multilayer barrier coatings (see details below in Section 5) [70]. The possibility to deposit conformal coatings over more complex, high-aspect-ratio substrates has also been evaluated. SALD proved to be very efficient in coating nanorod arrays at high deposition rates. Musselman et al. reported the deposition of conformal Al_2O_3 layers over electrodeposited ZnO nanorod arrays with a high rate of 0.12 nm/s. Mg- and N-doped ZnO conformal coatings were also deposited, showing a good electrical contact with the underlying nanorods, as shown by the application of the coated arrays in hybrid and quantum dot solar cells [74]. SALD was also used to coat high-aspect-ratio templates [47,75]. Sharma et al. demonstrated that SALD can conformally coat flexible alumina templates only when the right conditions are used depending on pore size. Optimized conditions were then used to coat porous oxide films for application as cathodes in lithium batteries. The results showed an improved capacity stability thanks to the Al_2O_3 coatings [47,76]. Moitzheim et al. have also recently shown that chlorine-doped amorphous TiO_2 deposited by SALD allows an increase in capacity when used as a cathode in a lithium battery [77]. Mameli et al. recently published a study in which the capability of conformally coating high-aspect-ratio porous substrates at high rates is evaluated. Because HT SALD is often performed at atmospheric pressure, the study is focused on the effect of pressure on the deposition quality and rate. Three key parameters are identified: pore aspect ratio, reaction probability, and precursor diffusion coefficient, which is linked to pressure. Simulations and experimental results show that in most realistic experimental conditions, the deposition is limited by precursor diffusion to the surface areas inside the pores. Nevertheless, the atmospheric pressure (S)ALD can allow HT deposition in porous substrates as long as high precursor partial pressures and molar flows can be achieved [75].

Some commercial SALD systems such as the cyclone tool by Jusung, the N333 tool by TEL, or the Olympia tool by Applied Materials are based on a rotating substrate holder that can accommodate several wafers. Upon rotation of the substrate holder, the wafers are exposed to the different precursors which are injected in different zones of the chamber, separated by inert gas regions. Given several samples are coated in the same run, these systems are considered as semi-batch ALD reactors as well and are mainly focused on the microelectronics industry. The same applies indeed to close proximity systems, when the samples to be coated are smaller than the injection head. Another batch-SALD approach is the one designed by van Ommen et al. for coating nanoparticles. Instead of the conventional fluidized bed reactor, they have designed a tubular reactor where the precursor and inert gas are injected in alternate sections of the tube. As the nanoparticles travel along the tube, an ALD coating is deposited. Given many nanoparticles are coated in each run, this system offers a HT [78].

While one of the main advantages of SALD is that it can be easily performed at atmospheric pressure, and even in the open air, attention must be payed when depositing materials which are suspected or known to be sensitive or unstable to oxygen or water. This is evident when dealing with organic semiconductors and hybrid perovskites such as the ones used in several optoelectronic applications. In these cases, SALD systems can be designed to be fitted in a globe box for research purposes, such as the one reported recently by Hoffmann et al. (see Fig. 18 in Section 5) [79]. Other cases are less obvious, but the consequences of processing in air can be very detrimental to the final properties of the deposited materials. This is, for example, the case of aluminum-doped ZnO (AZO), which shows much smaller conductivity values when deposited by open-air SALD as compared with the values obtained by sputtering, pulsed laser deposition (PLD), and even conventional ALD. This is because of the adsorption of oxygen species at the grain boundaries that result in an increase of the trap density. This, in turn, has a dramatic effect on the electron mobility of the films. Nguyen et al. have recently presented a new theoretical model where the effect of air-processing on the properties of polycrystalline AZO is exhaustively described [80]. Such issues are thus to be taken into account when performing SALD at atmospheric pressure or in the open air.

Finally, as in the case of batch ALD, modeling of the different SALD systems is an important step when optimizing the reactor design and deposition parameters. This aspect is discussed in more detail in the modeling section below (Section 4).

3.3. Reactor optimization

In this section, the possible gains in throughput that can be obtained by optimization of the geometry and operation mode of temporal ALD reactors are discussed. First, a discussion will be presented of the different gas transport phenomena that unnecessarily leads to longer purge times. Then, a particular architecture that addressed these different factors to improve cycle times by orders of magnitude, the parallel precursor wave (PPW) architecture will be discussed.

Gas transport is an essential part of the operating principle of temporal ALD reactors. Different gas transport phenomena affect the efficiency of the purge process, and therefore the required length of purge steps. To allow efficient and active purging process, the volume to be purged must consist of a conduit with an inflow of purge (i.e. neutral) gas and an outflow of a purge gas/precursor mixture. If the geometry of the reactor contains sub-volumes that do not allow inflow and outflow ('dead volumes'), the direct displacement of the purge gas/precursor mixture by pure purge gas becomes impossible in that volume. The only remaining mechanism for removal of the precursor is a gradual decrease of the precursor concentration by gas phase diffusion near the edge of the dead volume toward the pure carrier gas in the area which is flushed. This is a very slow and inefficient process.

In other occasions and depending on the geometry of the conduit and the flow conditions, a velocity pattern can develop where the gas flows in a vortex with a locally closed flow path. Such a vortex will effectively act as dead volume as the precursor/purge gas mixture is trapped in the vortex (even though no physical boundaries exist to retain it in this place). The creation of such a recirculation at generic geometrical features (such as forward and backward facing steps) has been studied extensively (see e.g. Ref. [81]). The key metric is the Reynolds number, which includes the density of the fluid (i.e. the gas pressure), the flow rate, and the geometry. The occurrence of recirculation effects depends on the operating conditions. As an illustration, Fig. 4 shows the simulated flow pattern in a gas conduit at low and high flow rate [82]. It can be seen that a vortex develops near the inlet at an increased flow rate.

As the flow rate is (by definition) zero on the wall of the gas conduit, some area with reduced flow velocity will exist near these boundaries. In the particular case of a cylindrical tube, the flow velocity profile becomes a Poiseuille distribution, i.e. a parabolic dependence of the amplitude of the flow velocity on the transversal coordinate. The effect of this reduced flow velocity near the edges on the purging of the precursor pulse depends on the relative importance of gas phase diffusion. If the characteristic length of gas phase diffusion is large with respect to the characteristic length of the flow velocity gradients, there will be a continuous transport between the zones having high flow velocity and the zones having low flow velocity. Thus, the effect of the non-uniformities in flow velocity on precursor concentration distribution tends to be smeared out. Conversely, there may be significant concentration gradients, and thus non-uniform purging. This leads to situations in which parts of the reactor with high flow velocities are completely purged, but the purge step must be continued to clear out also the areas with lower flow velocities.

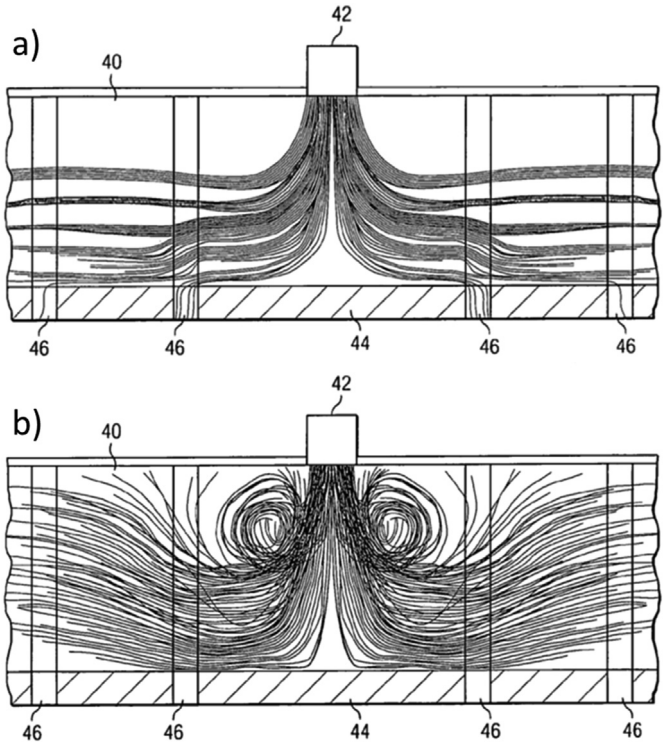

Fig. 4. Computational fluid dynamics study of the development of a vortex in a gas injection volume at different flow speeds. (a) Low flow rate, approximately 133 sccm. (b) High flow rate, approximately 1333 sccm [82].

A final factor that has to be considered is the effect of gas-surface interactions. In particular, the interactions between water vapor, which is very frequently used as an oxidant in ALD processes and surfaces of the gas conduit deserve attention. It was found that, as a function of relative humidity, water molecules may form a physisorbed layer of up to a few monolayers [83]. In an ALD process, where the relative humidity increases during the water pulse and subsequently drops again, it leads to a 'sticking' effect of the water on the surface. Thus, the presence of surfaces with a locally high relative humidity may result in smearing of the water pulse.

An example of how the above points can be addressed to speed up the ALD process can be found in the reactors designed by Encapsulix, which are based on the so/called *parallel precursor wave architecture*. The basic approach of this reactor architecture is to design and operate the gas conduit as a waveguide for the propagation of separated precursor pulses with minimal dispersion. Therefore, the entire design is optimized toward the creation of well-defined gas and vapor pulses in an appropriate sequence, and the transport of this sequence through the reaction space with minimal perturbation. The key enabling technology components are the gas dosing system, which generates the pulses and the injector [84], which create a uniform laminar gas flow in a rectangular reaction space. Fig. 5 shows a typical layout of a dosing system for a liquid precursor. The precursor is stored in a reservoir at a certain temperature T, resulting in a vapor pressure P_{vap}. The flow toward the reactor is determined by two valves, namely a fast pneumatic valve and a metering valve (some additional safety-related valves are not shown in this schematic). The result of a simulation of the time-dependent pressures P1, P2 in the volumes V1 and V2 is shown as well in Fig. 5 for a water source. Upon opening the dosing valve, the vapor which is in V1 almost instantaneously enters the reactor, resulting in a drop of the pressure P1 in that volume, and flow across the metering valve. During the pulse, evaporation from the liquid surface (S_{vap}) is not sufficient to compensate for this outgoing flux, and the pressure P2 will drop. Upon closing of the dosing valve, the pressure between the two volumes will equilibrate very rapidly, and the evaporation will restore the pressure to the vapor pressure in preparation for the next pulse.

Thus, the total amount of vapor injected (Fig. 6a) will be a non-linear function of valve opening time, doser geometry (V1, V2), precursor type and temperature, and position of the metering valve. A common characteristic is a rapid initial inflow, followed by a steadier flow gated by the metering valve.

This behavior is also found in the experimental data (Fig. 6b), with one additional caveat: the finite response time of the solenoid driving the pneumatic actuation of the dosing valves results in a time delay of about 10 ms between the arrival of the electrical signal and the actual opening of the valve. Thus, it can be seen that a vapor pulse of a sufficiently large number of molecules can be generated in 30–50 ms. In an R&D environment, it is desirable to vary the dose over a large range to explore different deposition conditions. For the example of Fig. 6, it can be seen that the water

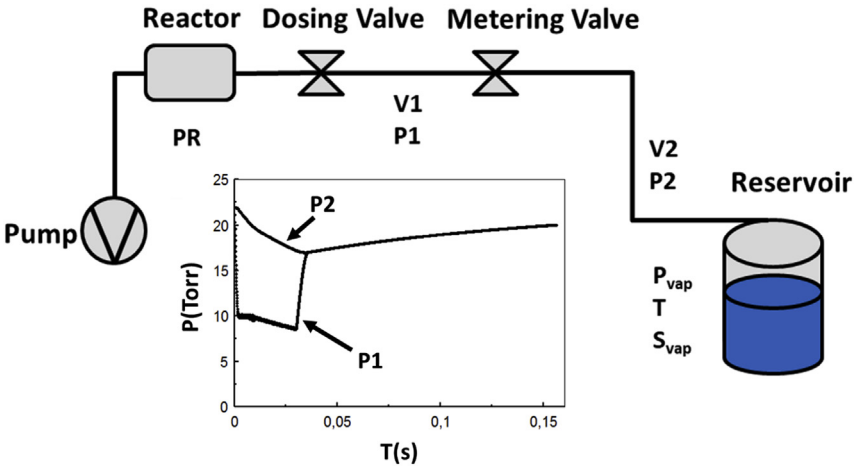

Fig. 5. Schematic of vapor dosing system for a liquid precursor used in the systems by Encapsulix. PR, reactor pressure; P_{vap}, precursor vapor pressure; T, temperature; S_{vap}, precursor surface area. The graph shows the simulated pressure (P1 and P2) in the two volumes (V1 and V2) during and immediately after a pulse.

vapor dose can controllably be varied between 3.5 μmol and 15 μmol using the dosing valve opening time and the metering valve position.

In a manufacturing environment, where the required dose does not vary, the optimal operation conditions are those in which the dose in the initial volume V1 corresponds to the required dose. This leads to a stable, fast injection of the required quantity of precursor. The PPW method utilizes a modular system of gas injectors (Fig. 7a) allowing the creation of a highly uniform laminar flow in the reaction space at very high flow speeds. As a result, the transport of the precursor pulse shows very little dispersion. This is illustrated in Fig. 7b, which shows a computational fluid dynamics (CFD) simulation of the isoconcentration contours after propagation of a 20 ms trimethylaluminum (TMA) pulse in a 600 mm long reaction space. It can be seen that the precursor propagates rapidly through the reactor. At this point, the reaction space is ready to receive the next precursor pulse, even before this pulse has completely gone through it.

As a result, the purge times can be reduced drastically. For example, a thermal Al_2O_3 process at 80 °C, for OLED encapsulation at manufacturing level onto industrial size glass substrates, has been operated stably in the ALD regime for tens of thousands of depositions using TMA purge times around 150 ms and H_2O purge times around 600 ms for a total cycle time of less than 1 s. This is in strong contrast to conventional practice in ALD. For example, applying the same process chemistry and temperature in a conventional ALD R&D can require purge times of 5 s and 20 s for the TMA and H_2O purge times and a total cycle time of 28 s [85]. Similarly, in Ref. [86], it is recommended to flow an amount of gas corresponding to twice the volume of the reaction space (defined in a particular fashion) in between two precursor pulses to ensure stable operation in the ALD regime. In contrast, in PPW systems, operation in the ALD regime is obtained with an amount of neutral gas corresponding to less than 0.2 times the reaction space.

Similar reactor optimizations are also applied in other commercial systems intended for production. This is the case for example of the Pulsar® XP Reactor from ASM, in which the reactor chamber and source delivery system have been optimized for precise gas-flow dynamics and minimum purge times, thus providing advanced process control and high film purity and uniformity. And as mentioned above, reactor optimization is a key point toward decreasing the cycle time in batch reactors.

3.4. Process engineering

Process modifications with respect to the standard ALD process have been achieved with reactors specifically designed for such process modifications [87,88]. However, such results can be achieved, to a lower extent, in most ALD reactors. When tuning the process, one has to keep in mind three aspects which are the

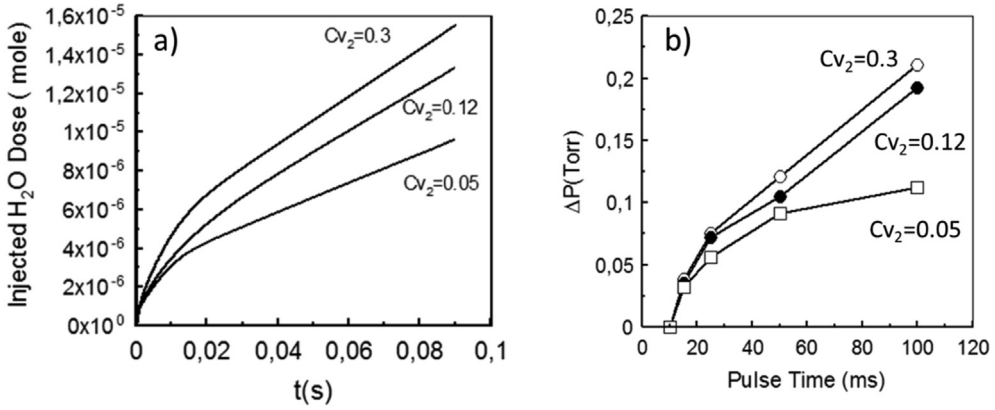

Fig. 6. a) Simulated of precursor doses injected vs. time after valve opening, for different dosing valve opening times; (b) experimental injected doses expressed as variation in pressure vs. time after valve opening, for different dosing valve opening times.

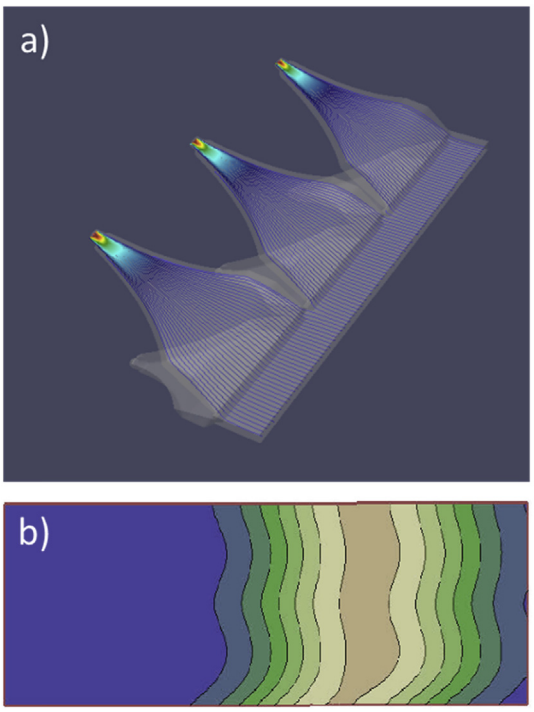

Fig. 7. a) Computational flow dynamics simulation of the gas injectors in the Encapsulix PPW system; (b) precursor concentration isocontours after propagation of the precursor pulse in the reaction space. PPW, parallel precursor wave.

precursor condensation, unwanted CVD reactions, and insufficient exhaust of the reaction by-products. Precursor condensation takes place on cold parts of the reactor or when the precursor vapor pressure in the reactor is too high. It results in the deposition of the material on the walls of the reactor, in turn leading to the generation of particles or flakes [89]. Unwanted CVD reactions are observed when purge of the precursor or reactant gas is not sufficient and the two meet in the reaction chamber, and it results in the generation of particles and defects in the deposited material [42,89,90]. The insufficient elimination of the reaction by-products leads to poor characteristics of the deposited material because of the trapping of unwanted species in the deposited layer [42,89,90]. Many different aspects of the process can be tuned to increase the deposition rate in ALD. However, most of them are related to the precursor or reactant gas chemistries, and the increase of the deposition rate is limited by the kinetics of the absorption reactions. Such parameters are for example precursor partial pressure, flow speed, pumping speed, etc. Few parameters can enhance the deposition rate further, including precursor chemistry, the addition of catalyst species, deposition pressure variation, removal of purges, and plasma enhancement[42,89–91]. The effect of modifying three of these parameters on deposition rate are presented here: pressure variation, elimination of purges in purge-less ALD mode, and plasma enhancement. Each has advantages and limitations, examples used here correspond to the best-case scenario of what has been reported in the literature.

3.4.1. Pressure variation

Similarly, to performing a CVD-type process, if bursts of the precursor to be deposited are used (Fig. 8), good conformality can be achieved at a high deposition rate and great repeatability. Pulsed pressure CVD (pp-CVD), as it is called, uses the expansion of the precursor in a short time to allow a good coverage of the substrate [87,92], as opposed to ALD, where precursors are injected in a viscous flow. The burst pressure is then followed by a pump-down phase to remove the reaction by-products and unreacted species.

A precise control of the quantity injected leads to deposition of thicknesses close to the monolayer at a deposition rate close to the ALD deposition rate, i.e. 1–5 nm/min [92]. But an increase of the injected quantity per cycle leads to a deposition rate ranging from 10 to 100 nm/min, with limited impact on conformality and material properties. One of the main drawback of this approach is that it has mainly been used for the deposition of monoatomic materials, such as Pd, Co, W, Cu, etc. [93] The pp-CVD approach has also been used in batch reactors and has shown edge coverages of more than 90% for aspect rations of 32 [23].

3.4.2. Removal of purges

In a standard ALD cycle, the purging time represents at least 50% of the process time. Hence suppressing the purges between each injection would lead to higher deposition rates. This can only be done when the chemistry prevents the reaction between precursor and reactant in the volume of the chamber. As an example, such an approach is found in the so-call fast atomic sequential technique (FAST), which is equivalent to 'pulsed-CVD' or 'purge-less ALD'. Maximal separation of the precursor and reactant can be achieved by the use of dual-channel showerhead, such as what can be found in some CVD tools. In such tools, by pulsing the precursor and reactant gas, without or with an overlap of the pulses, one can obtain deposition in a CVD regime or ALD regime. Fig. 9 shows different pulse sequences that can be performed and that correspond to the different deposition modes discussed.

To illustrate the effect of the different pulse sequence on film deposition, Fig. 10 presents the evolution of the deposition rate of TiN using CVD, ALD, and FAST techniques in the same deposition reactor [88]. For all three techniques, deposition was achieved using an ALD and CVD compatible precursor: tetrakis(diethylamido) titanium and NH_3 reactant gas, at the same deposition temperature. In a CVD mode, the precursor and the reactant are sent together to the reaction chamber and react on the heated wafer. In the ALD mode, purges allow desorption of precursor and elimination of reactant gas excess altogether with the reaction by-products. In the FAST mode, the pulses are gap-less and overlap-less, with a minimum variation of the pressure in the chamber to allow a continuous flow above the substrate.

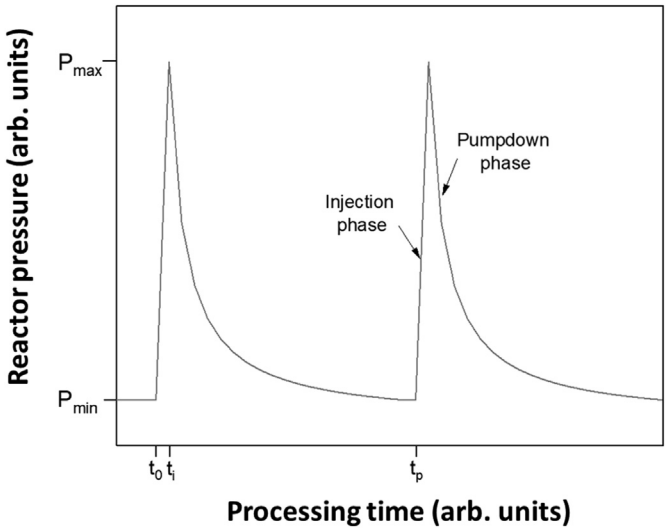

Fig. 8. Evolution of the pressure in the reactor during a pulsed pressure CVD deposition. CVD, chemical vapor deposition.

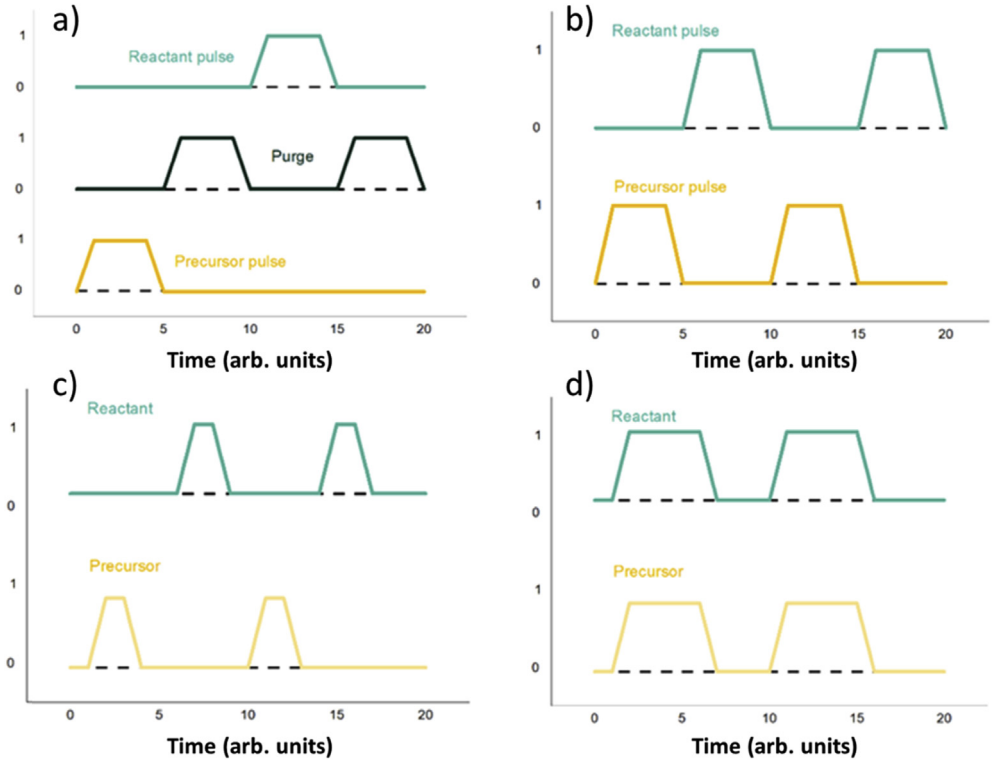

Fig. 9. Sequence of precursor pulses and purges in different operation modes: (a) ALD mode, (b) FAST mode, (c) FAST ALD–like mode, and (d) FAST CVD–like mode. FAST, fast atomic sequential technique; CVD, chemical vapor deposition; ALD, atomic layer deposition.

Removing the purges of the ALD technique resulted, in this case, in a 4-fold increase of the deposition rate, while keeping the linear deposition rate from the first step. This deposition rate is still twice slower than the CVD mode but allows a control of the deposited thickness down to the angstrom (the deposited thickness per cycle) and a higher conformality than CVD or pp-CVD [88,94]. In addition, the process obtained has a 23% lower activation energy than the MOCVD technique [94], resulting in a lower minimum deposition temperature, i.e. down from 250 °C to 200 °C. Furthermore, lower resistivity of the TiN metal layer was achieved, resulting in a resistivity closer to the one obtained with ALD deposition (Fig. 10b). Other materials have been tested, such as TaN, ZrO_2, or Cu, and behaved in similar fashion. However, some precursors led to no deposition (such as tetraethyl orthosilicate [TEOS] for SiO_2 deposition) or formation of powder (such as TMA for Al_2O_3 deposition).

3.4.3. Plasma enhancement

In some cases, the reaction between the precursor and the reactant gas only happens in a well-defined temperature window. In that case, a plasma can be used to initiate the reaction. For example, ALD deposition of Ta_2O_5 from $Ta(NtBu)(NEt_2)_3$ (tris(diethylamido)(*tert*-butylimido)tantalum, TBTDET) and O_2 is obtained for a substrate temperature higher than 300°C. Below that temperature, the oxidation of the TBTDET is not observed, hence no nucleation sites are created during the O_2 pulse for further growth of the layer. Owing to this well-defined deposition temperature window, one can use O_2 not only as a reactant gas but also as a purging gas, permitting the decrease of the required purging time [95]. The oxidation step of the precursor will be thus limited by the plasma-on time. Fig. 11 shows a comparison between the standard plasma enhanced ALD (PEALD) process with the engineered

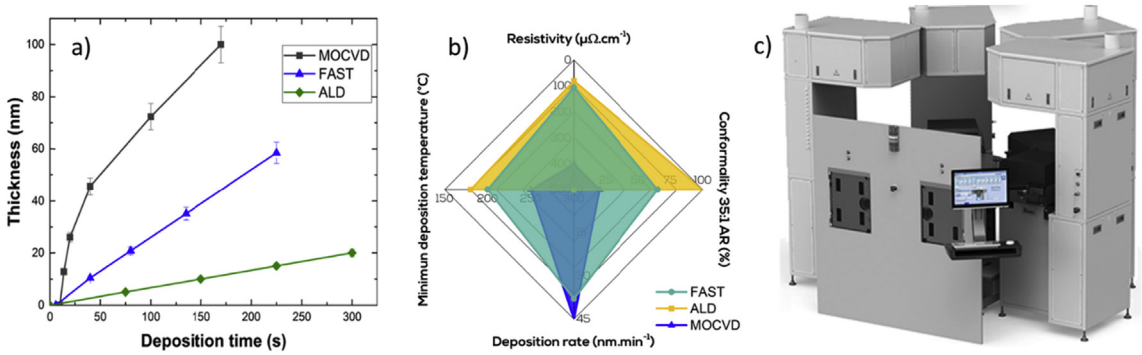

Fig. 10. (a) Variation of TiN deposition rate from TDEAT and NH_3 by ALD, MOCVD, and FAST techniques. (b) Comparison of ALD, CVD, and FAST deposition techniques for the deposition of TiN using the same precursors and temperature. (c) FAST reactor cluster from KOBUS used to perform the deposition of TiN in the three different modes. FAST, fast atomic sequential technique; CVD, chemical vapor deposition; ALD, atomic layer deposition; TDEAT, tetrakis(diethylamido)titanium; MOCVD, metalorganic chemical vapor deposition.

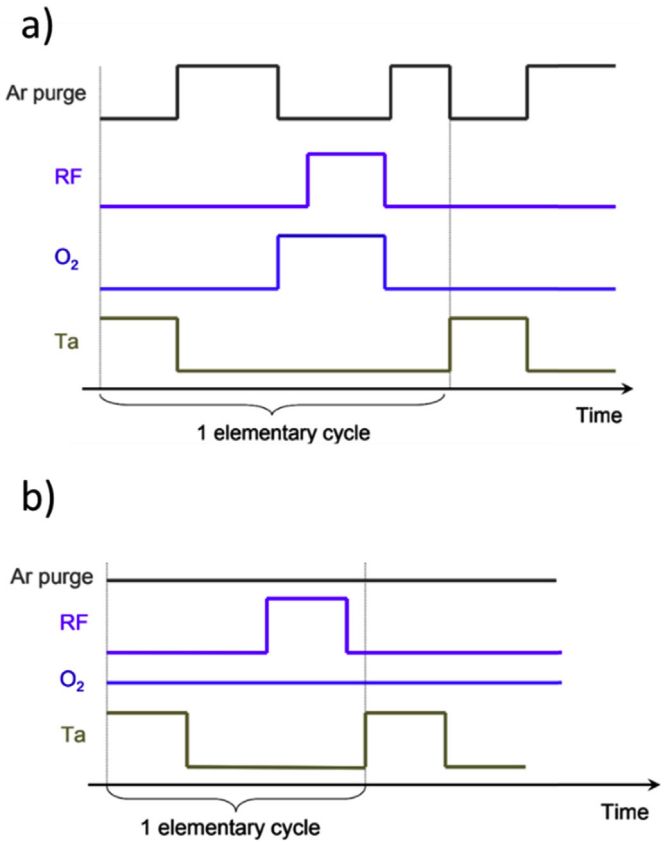

Fig. 11. Comparison of PEALD elementary cycle (a) and engineered-PEALD elementary cycle (b). RF, radio frequency.

process. As one can see, the elementary cycle in the case of the engineered process needs many fewer steps.

Using this approach, the elementary cycle time is reduced by up to 20%, resulting in a deposition rate of up to 4 nm/min. This approach is suitable for precursors which have no or limited reaction with the reactant gas in a temperature window matching with the temperature of self-limiting surface saturation required for ALD deposition (i.e. ALD window).

Plasma enhancement can also be paired with the FAST technique discussed above. In that case, precursors which do not present a self-limiting surface saturation step (as needed for ALD deposition) can be used. Fig. 12, shows the GPC and growth rate of SiO_2 deposition from TEOS and O_2 plasma in a purge-less ALD mode, with cycle time ranging from 0.2 up to 1.2 s (half of the time is used for TEOS injection and the other half for plasma O_2 activation).

This figure clearly highlights the shift from an ALD regime, i.e. a GPC which is limited to a monolayer of SiO_2, between 0.2 and 0.8s, to a CVD regime for longer cycles, in which the GPC increases linearly with injection time.

Process engineering can also be tackled in SALD reactors. In particular, in close proximity reactors where the deposition head can be adjusted mechanically, the gap between sample and head can be adjusted so that crosstalk of precursors in the gas phase above the surface is allowed. For precursors and temperatures giving rise to chemical reaction, this means that a CVD-like mode is obtained in addition to the ALD process taking place on the surface. While CVD growth could compromise film conformality, for featureless, flat substrates, it is not dramatic to allow this CVD component. These conditions are attractive for device production

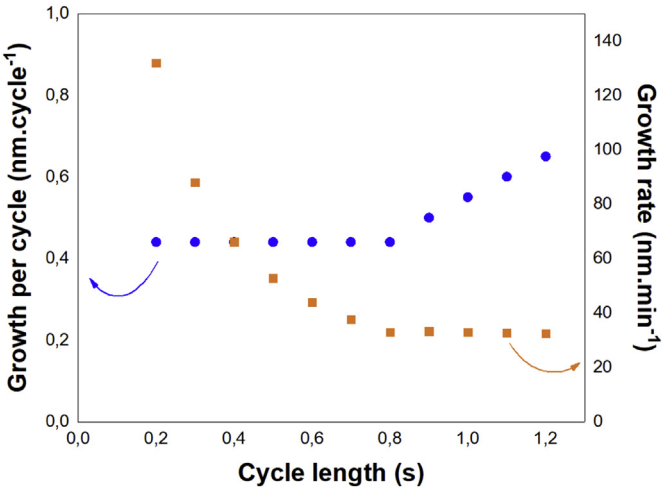

Fig. 12. Evolution of the SiO_2 growth per cycle and growth rate depending on cycle length in FAST deposition mode. FAST, fast atomic sequential technique.

as higher rates are obtained, while still producing smooth, pinhole-free films at modest temperatures. Obtained thicknesses are as well proportional to the number of SALD cycles, which allows a precise control over thickness, as in conventional ALD mode. Thus, homogeneous, high-quality (ALD-like) films can be achieved at around twice faster deposition rates by using this CVD-like approach, as has been shown for ZnO [53,74,96]. The same approach has also been shown on high-aspect-ratio samples, in particular, to coat ZnO nanorod arrays. Musselman et al. have recently shown that higher deposition rates (one order of magnitude) can be achieved to by working in CVD-like conditions, reaching depositions rates of 7 nm/min for Al_2O_3 at 150 °C, using TMA and H_2O [74]. In the same article, the authors show that the films obtained have similar quality than films obtained in ALD conditions, allowing the fabrication of functional devices. In an industrial context, running SALD in CVD-like mode would have to be optimized so that mixing of precursors only takes place above the surface of the sample and not on the deposition head or other parts of the reactor, so that maintenance costs can be kept at a minimum.

4. Modeling: a key tool in high throughput

As discussed above, HT deposition techniques push the limit of the ALD basic operating window to such levels that proper design of the different aspects, i.e. chemicals, substrate surface states, inlet and reactor, and processing choices, are to be considered in their mutual and complex interplay. Compared with traditional chemical deposition techniques, such as CVD or MOCVD, typical ALD conceptually reduces drastically the chemical complexity of the overall deposition process, hindering all potential gas phase reactions and projecting itself into more or less one-step self-saturation chemical reaction with the surface. This apparent simplicity, making it a well-defined model system, has attracted considerable attention from a purely theoretical perspective. Since the beginning of the century, atomic scale modeling, mainly density functional theory (DFT) calculations has established itself as a remarkable tool to provide quantified ALD chemical reaction paths, from both thermodynamic and kinetic points of view [97–102]. From these insights, macroscale and mesoscale models have been derived: (i) using Kinetic Monte Carlo (KMC) techniques to highlight collective behaviors and structuring of a limited number of ALD layers at the atomic scale [103–105], (ii) using mechanistic

kinetic models at the continuum scale [106–108], more adapted to direct industrial engineering usage. Finally, the consideration of fluid dynamics equations has allowed to tackle issues related to the scale of the reactor [109,110]. Overall, all these simulation levels draw a hierarchical bottom-up methodology in which each level can provide essential data to higher modeling levels, in terms of time duration and system size that can be simulated. In practice, a complete loop from atomic scale fundaments to reactor scale simulations has only been partially accomplished to date, as each modeling level suffers from intrinsic difficulties in addition to coupling issues between levels.

Owing to its applicative interest in microelectronics applications, alumina deposited by TMA/H_2O ALD corresponds to the most studied and therefore most illustrative example discussed in the literature. It is often considered as a model system to explore ALD processes. Note that at the scale of the individual molecular interaction/reaction, there is strictly no difference between classical ALD and HT ALD. After two decades of research effort, a rather satisfactory inventory of TMA-related interactions has emerged. The results exhibit an infinitely more complex picture than it was initially expected: self-interaction in the gas phase with formation of TMA dimers, strong variation of decomposition activation barriers, ligand exchange mediated by proton transfer, the effect of co-adsorption, and hydroxylation, among others [102,111–113]. In addition, the initial surface offers drastically different chemistries than the steady-state growth chemistry after the initial surface coverage is reached. This generally translates into an incubation period in the GPC profile but leads also to deviations from the ALD window and specific structuring of the interfacial region.

KMC and mechanistic calculations, while they are by far less documented, are crucial modeling steps to give an overview and quantify the relative importance of an ensemble of very diverse elementary mechanisms (adsorption, surface configuration, reaction, and migration) such as described by DFT calculations. For instance, Travis and Adomaitis have provided a reaction factorization technique that allows the separation of different classes of mechanisms as a function of their kinetic time scales [106,114]. Early KMC results from Mazaleyrat et al. have provided evidence that cooperative effects (so-called densification) are mandatory to achieve proper structuring and the coverages observed experimentally [104]. These modeling steps are also essential to get feedback information for further DFT investigations of fundamental mechanisms. Interestingly, Poodt et al. have developed a kinetic model specifically dedicated to SALD, making a direct relation to the GPC. Their work underlined the role of the water reaction and underlined that diffusion of precursor to the substrate is rate limiting [115].

CFD is probably the most important growing field in providing predictive tools to HT ALD processing. At this level of theory, all aspects of ALD can be envisaged within an integrated multiscale/multiphysics approach. But primarily, the objective is to address transport phenomena in the chamber, which is crucial to the determination of partial pressures, dosing and precursor crosstalk, precursor exposure or purge/pumping durations, and temperature, as a function of reactor geometry. Within CFD simulations, all these aspects can be analyzed to obtain the desired uniformity over large or distributed substrates (batch ALD) and with good conformality of the deposited layers. Holmqvist et al. wrote a series of papers dedicated to the setting up of a comprehensive modeling framework dedicated to reactor scale modeling [116–118].

CFD simulations with neutral gases are currently used to properly design the reactor chamber at the industrial level to maximize the deposition rate, as has been detailed above [119]. This allows recirculation effects, turbulences, and non-uniform flows to be readily anticipated and corrected, thanks to systematic modification of the reactor chamber and inlet geometries. 3D transient simulations on batch ALD were performed by Lankhorst et al. to evaluate the deposition parameters necessary to deposit HfO_2 (TEMAH, $Hf[N(C_2H_5)(CH_3)_3]_4/H_2O$) on high-aspect-ratio trenches [120]. Gakis et al. have proposed to couple two 3D CFD models to account for both the gas flowing through the feeding inlet and the gas transport over the reactor chamber [121]. The work identifies non-uniformities in the concentration of TMA over the substrate and temperature distribution due to the purging flow positioning from the substrate. Note that no surface reactions are considered in this work.

Obviously, the level of understanding of precursor transport and, above all, precursor surface interactions is far from being mature for the majority of processes and materials. In addition, the overall complexity of chemical mechanisms, such as in the case of TMA/H_2O ALD, cannot be fully implemented for computational reasons (resources and formulation complexity). A simplified formulation was proposed by Yanguas-gil and Elam for classical ALD [122], with potential extension to more complex physicochemical processes. Xie et al. were the first to provide CFD simulations coupled to the gas/surface chemistry of ALD deposition of alumina via TMA/H_2O exposures [123]. These authors provided basic information on the effect of temperature and pressure, highlighting differences in sensitivity depending on surface species.

Concerning HT techniques, Deng et al. proposed a numerical framework for solving SALD issues dealing with a simplified laminar type of rate model to account for surface reactions [124]. The authors discussed the separation of gases, and the mass fraction of precursor is shown to be of crucial importance to perform HT deposition. The fluid dynamics at the gap region in their close-proximity SALD model system are discussed in detail to arrive at proper gas separation and diffusion (low Péclet number) in the desired reaction zone. Pan et al. further proposed to optimize the gap size between the gas cylinders and the moving wafer belt of a SALD reactor [125]. They demonstrated that while intermixing can be reduced by increasing the gap, it also affects the growth rate by lowering the self-saturation level. Also, the authors unravel the role of substrate temperature which favors intermixing and increases growth rate. Finally, the simulations unraveled that a full cycle could be realized within a few tens of ms which would allow growth rates of a few nm/s.

Another important factor to take into account when designing SALD reactors and when optimizing deposition conditions is the possibility of precursor entrainment from one region of the reactor to another in which the second precursor may be present. SALD reactors involve the fast movement of the substrate across the different zones where the precursors and inert gas are present. Because there is always a boundary region where the relative velocity of a gas and a surface is 0, it means that precursor molecules near the substrate surface could be carried along with the substrate, giving rise to higher GPC than expected. Levy et al. used finite element modeling of gas flows to evaluate the effect of substrate scanning speed on precursor entrainment in their close-proximity system. The calculations were performed for scanning speeds of 0.5 m/s and 3.5 m/s. The results clearly show the influence of substrate speed, but in both cases, the precursor is confined to areas that prevent crosstalk with the second precursor, thus ensuring ALD deposition mode. (The result of a simulation showing the effect of precursor entrainment in a close-proximity SALD system is shown in Fig. 13) [54]. In another report, Maydannik et al. observed an anomalously high deposition rate in a system designed for moving flexible substrates. While the authors initially explained the deviation form ALD behavior as due to entrainment of the precursor [126], in a later report, the same authors presented a study on the gas entrainment effects on their reactor using helium as a tracer gas. The results showed that no entrainment was indeed taking place, and water condensation was suggested as an

alternative explanation [127]. This shows the importance of using an accurate model when simulating an ALD reactor.

5. Case study: HT ALD for encapsulation

In this section, we give an overview on how HT ALD is being developed for an application in which film quality, deposition rate, and cost are very important aspects, namely, thin-film encapsulation of air-sensitive devices like OLEDs. There has been a trend in the microelectronics industry to integrate several types of high-performance nanoelectronic devices (e.g. sensors, displays, etc.) into CMOS-type integrated circuits ('More than Moore'). Many of these devices, such as microelectromechanical systems (MEMS), sensors, OLED displays, LED components, thin-film batteries, and memories, can be based on complex structures of new materials like for instance transparent conductive oxides for PV [128] or organic semiconductors (π-conjugated small molecules or polymers) for OLED [129]. Unfortunately, many of these new materials are extremely vulnerable to degradation by atmospheric gases such as water vapor and require extreme protection using high-performance thin-film barrier as encapsulation. As the device reliability is critical in many applications, OLED, in particular, requires encapsulation techniques showing an ultra-high barrier (UHB) grade. These barriers are usually characterized by their water vapor transmission rate (WVTR) which has to be of the order of 10^{-6} g/m^2/day for the OLED display industry to ensure a lifetime of 10 years [130]. This is today accomplished in a mass production environment by using glass encapsulation where a thick glass lid is fritted around the perimeter of the rigid glass substrate using a laser [131] or by using ALD-deposited barrier films in OLED microdisplay technologies [132]. As a reference value, plastic sheets commonly used in food packaging but also planned to be used as flexible substrates for the display industry, generally have a WVTR value of only 1–10 g/m^2/day, because of their intrinsic very poor barrier properties against oxidizing gases [133]. Usually, in the food packaging industry, Al barrier films are deposited onto R2R lines so as to reinforce the WVTR of the plastic pouch [134]. Performances of barrier materials are however limited because of the use of PVD processes in non-clean room conditions (process cost must be ridiculously low), at the high-speed motion of rolls.

Contrary to food packaging, the application of barrier films in OLED display technology also involves the mastering of killer defects during the steps of realization of the encapsulation layers. This means that R2R and non-clean room conditions of the process are not suitable. This is because the UHB level for the barrier implies that the number of defect/surface unit must be extremely low [135]. If this condition is not fulfilled, undesired black spots will appear onto the emitting surface of the corresponding OLED device [136]. This assertion is particularly true for OLED-based microdisplays for which the image on the display is enlarged by an optical engine system [137].

Obtaining UHB properties using PVD techniques to deposit the dense inorganic barrier layers (e. g. oxide or nitride) to protect OLEDs requires the implementation of hybrid multilayer structures, by alternating dense inorganic layers and extra polymer decoupling layers [132]. This kind of architecture allows to decouple pinhole defects inevitably present in PVD or PECVD-deposited inorganic layers [132]. The improvement of the barrier properties results from the lengthening of the diffusion path of the oxidizing gas molecules (O_2, H_2O) in these hybrid structures (principle of the tortuous path). The resulting reduction in the diffusion coefficient considerably reduces the WVTR and also increases significantly the lag time required to reach the steady state WVTR [132].

Affinito et al. obtained the first transparent multilayer system using a three-layer hybrid structure of the kind [polymer/PVD Al_2O_3/polymer] obtained by PVD on a PET substrate and called PML for polymer multilayer process and developed in the early 80's at General Electric capacitor's division [138,139]. The thick polymer layers were made by vacuum evaporation (e-beam) of a dedicated monomer (blend of acrylate derivatives) crosslinked in situ, as thin films, by UV exposure. The monomer forms a liquid film and fills the pinhole defects of the inorganic film, before being crosslinked. By increasing the number of dyads (polymer/inorganic unit), WVTRs of less than 5×10^{-3} g/m^2/day have been measured in this study. The same thin film encapsulation has been applied to OLED. Based on the measurement of the lifetime of the encapsulated

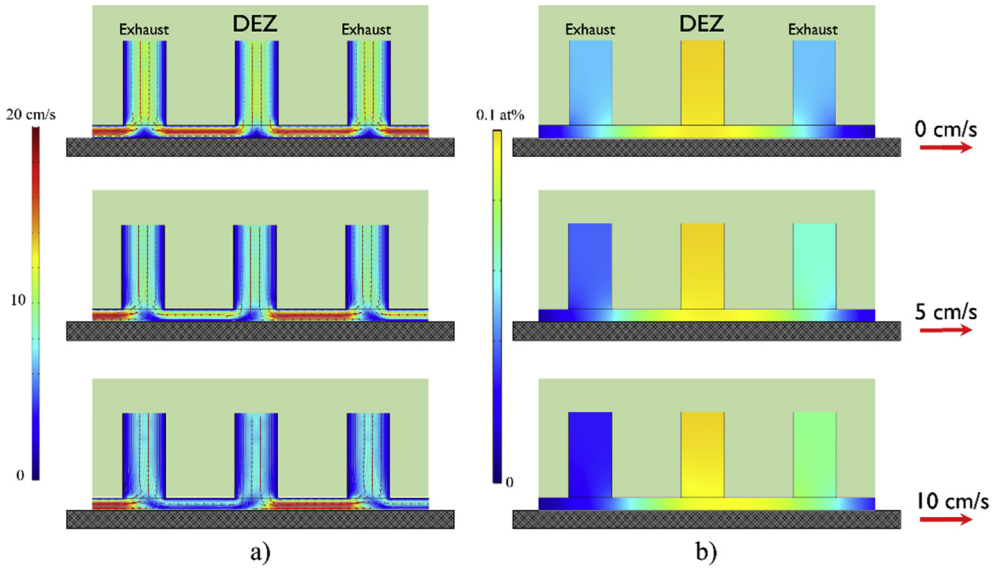

Fig. 13. Spatial distribution of (a) precursor velocity and (b) precursor concentration above the substrate for the deposition of ZnO from diethyl zinc (DEZ) with a close-proximity head such as the one in Fig. 2. Only the cross-section views including a DEZ inlet and two exhaust inlets are shown here. The blue color corresponds to low velocity/precursor concentration, while red or yellow color corresponds to high velocity/precursor concentration. As it can be appreciated, more precursor entrainment takes place as scanning speed increases.

OLED, authors estimated a WVTR of 10^{-5} g/m^2/day [140]. This process was originally proposed by the US company Vitex, a company recently acquired by Samsung in 2011. It turns out that the multilayer inorganic/organic structures made by PVD face some problems to allow mass production, probably because the sputtering deposition can alter the fragile OLED circuits and because of some reproducibility issues originating from the difficulty of controlling the defect distribution in the inorganic layers. One way to circumvent the issue related to pinhole defects in the inorganic barrier layers is to use alternative defect-free deposition techniques like ALD.

Indeed, a great feature of the ALD technology is that it allows the production of inorganic layers that are practically free of defects over a wide temperature range (from ambient to about 300 °C). Thermal ALD, in particular, is preferable to other thin film deposition technologies (PECVD, PVD) because it does not produce particles. Plasma enhanced-ALD can allow the realization of very good quality layers, but the process window control is probably more drastic because of the use of a plasma that may generate particles [141]. In the case of thermal ALD, the particle generation control is easier in real ALD mode (CVD modes have to be avoided): the particle levels can, however, increase after a certain number of runs when gas lines and walls in the reactors are saturated, and therefore the reactor starts to flake. This particle contamination is obviously a key feature of ALD reactors and a fortiori must be considered in fast-ALD processes.

It is common to assimilate the ALD technology to the chemistry of the couple TMA and water to produce Al_2O_3 films. One of the main reasons lies in the general properties of the TMA molecule, which is a stable, highly volatile (high vapor pressure at ambient, 13 Torr [142]), and reactive organic compound. The TMA temperature process window is important and varies between room temperature and approximately 300 °C. This material deposited by ALD is really adapted, from a scientific and technological point of view to the realization of atmospheric barriers for the encapsulation of air sensitive devices like OLEDs. Other materials can be deposited in an easy way, as for instance ZnO or ZnO:Al, from the highly reactive and stable, with a large temperature processing window, diethyl zinc (DEZ) molecule and water. These model type molecules can easily be processed in a fast ALD environment, as this has been already shown in most of the publications related to HT ALD (mainly SALD) processes. Alternatively, other precursors with a low vapor pressure at ambient temperatures must be heated up in their canister and all along the line to the ALD reactor [33,41,143]. While it is not always easy to keep a constant processing window in standard, cross-flow reactors, this aspect has to be considered when comes the time to implement such processes into HT ALD systems.

5.1. Alumina barrier layers deposited by ALD at low temperature

The main characteristics of Al_2O_3 ALD are (i) a wide temperature process window (no degradation in gas phase) [85]; (ii) a very low critical thickness [144]; (iii) Al_2O_3 has excellent optical transmission in the visible range, an important quality for devices through which optoelectronics is performed (e.g. photon emission for OLEDs of the top-emitting architecture type); and (iv) a good general adhesion to the substrate it is deposited upon. Inversely, problems related to the use of Al_2O_3 layers by ALD for encapsulation of fragile devices are as follows: (i) the purely thermal low temperature deposition show very long deposition times when water is used (water has high sticky coefficient and thus at temperatures around or below 100 °C, it requires extremely long purges to avoid CVD mode); (ii) there is usually a high residual content of C and -OH in the final layer [85]; (iii) oxidizing reagents (H_2O, O_3 or O_2 plasma) are not intuitively suitable for use with fragile organic circuits like OLED, which intrinsically need to be protected from these gases and can react to large amounts of water oxidant, as demonstrated [145]. If one has to implement HT ALD onto OLED, all those characteristics must be of course considered.

A thin layer of Al_2O_3 by ALD has intrinsic qualities perfectly suitable for a gas barrier function; the layer is dense with intrinsically a low level of pinhole features. It has been demonstrated that thin Al_2O_3 films deposited by ALD at low temperature (<120 °C) can reduce the WVTR of plastic substrates by orders of magnitude below the intrinsic WVTR of the raw plastic substrate: WVTR values as low as 1.7×10^{-5} g/m^2/day at 38°C/85% RH were measured for an Al_2O_3 oxide film thickness of only 25 nm, onto PEN [146]. Recently, the OLED research group at CEA-LETI calculated a value of 2×10^{-5} g/m^2/day at 85 °C/85% RH based on the use of a fluorescent test to monitor the degradation of the Al_2O_3 barrier, made in a standard cross-flow reactor (Savanah 200, Veeco Instruments) [130]. Good performances (unpublished) have been obtained onto an Infinity 200 system from Encapsulix, using the same organic fluorescent film as the atmospheric sensor, as depicted in Fig. 14. Details of the procedure can be found in Ref. [147].

It can be seen on the figure that the unencapsulated molecule degrades very quickly because of photooxidation under the UV irradiation (fluorescence intensity divided by 20 after 10 min), while it retains a high level of fluorescence when it is encapsulated with a single 25 nm thick Al_2O_3 barrier. Most importantly, there is no difference in degradation rates between the slow ALD system (30 s/cycle) and the fast ALD one from Encapsulix (3 s/cycle). These good results were also obtained with an OLED sample, as shown further in the text.

One of the main problems with Al_2O_3 films deposited at low temperature lies in their high sensitivity to moisture. As a consequence, additional barrier layers must be used to passivate the Al_2O_3 film. This case scenario has already been shown by several groups using rapid SiO_2 by ALD [148] or SiO by PVD [130]. Besides, it has been shown that the critical thickness of Al_2O_3 ALD films could be as low as 5 nm thick on polymers, which turns out to be a very low value compared with what is commonly measured for inorganic films deposited typically by PVD or PECVD, as for instance for

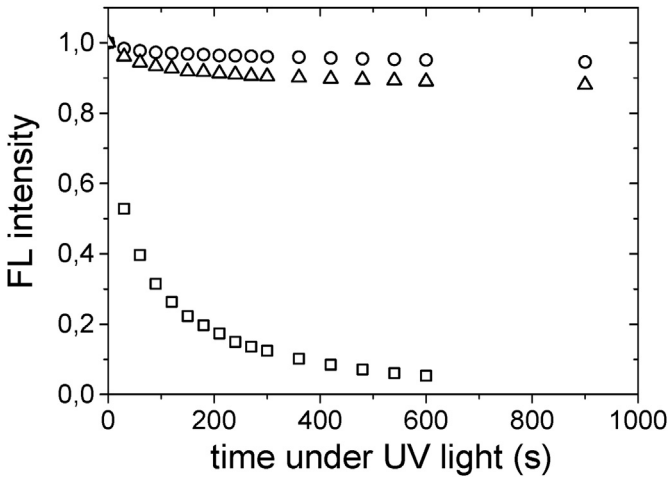

Fig. 14. Evolution of the normalized fluorescence (FL) intensity, under constant ultraviolet (UV) light and in laboratory atmosphere, of (squares) an Alq_3 thin film and an Alq_3 thin film encapsulated with 25 nm Al_2O_3 deposited by low-temperature ALD (90°C) in (triangles), a Savanah 200 standard cross-flow reactor (30 s/cycle), and (circles) in an fast-ALD Infinity 200 PPWR system from Encapsulix (3 s/cycle); thickness of Alq_3 films is 100 nm. Source: CEA-LETI. ALD, atomic layer deposition; Alq3, tris-(8-hydroxyquinoline)aluminum.

SiO_2 [149]. Therefore, if one combines ALD of Al_2O_3 with another material deposited by other faster processes (sputtering or PECVD), it means that thin Al_2O_3 (~5 nm) coated by thick PVD or PECVD films should theoretically be sufficient to ensure a UHB level. Of course, this low value for the critical thickness of ALD films is substrate-dependent and may, therefore, vary while the implementation of PVD or low-temperature PECVD is not an easy task onto fragile circuits like OLED. The mechanical stress in PVD films is high, and therefore this strategy may show some limitations for flexible applications. Finally, conformality of deposition technologies could be a hurdle also, in particular for PVD; however, it could be a viable solution for rigid displays and PVs where surfaces to be coated are fairly planar. In any case, if one can find a suitable combination material to coat on the very thin 5 nm Al_2O_3 layer, the realization of the ALD layer by a fast ALD technique, together with the high-speed deposition of the passivation layer, will probably help to lower down the production costs of display or PV panels.

There are a couple of examples of HT ALD processes using TMA as precursor to deposit Al_2O_3 as a thin-film barrier to protect plastic films. However, there are almost no publications describing the encapsulation of OLED circuits by fast ALD technologies or devices of the kind, based on organic semiconductors. We will show later on in this work some results we had in-house, at CEA-LETI, regarding the encapsulation of OLED using the HT ALD Infinity reactor from Encapsulix. The literature describing materials deposited by HT ALD as atmospheric barrier layers is mostly oriented toward the characterization of the barrier materials onto plastic films. Few references provide WVTR measurements, which is the value of the interest in this application, considering that this parameter is crucial for OLED technology and the one used by the display industry. Table 2 gives a (non-exhaustive) list of recent works on the development of Al_2O_3 barrier films deposited by SALD.

Despite some discrepancies in the measured WVTR values, it can be seen that interesting values of WVTR have been reported, down to ~10^{-6} g/m^2/day, which is the typical target value for OLED-based displays. Discrepancies between the measured WVTR values can originate from different factors: the level of particle contamination is obviously different in each case and the barrier quality of the barrier material may differ from one substrate to another. One can conclude that SALD processing of barrier layers could technically be a method of choice to encapsulate organic circuits like OLED, organic photovoltaics (OPVs), or organic thin film transistors (OTFTs) but the feasibility of a 10-year lifetime organic circuit based onto HT ALD as barrier layer technology has still to be proven in a mass-production environment.

Unlike the few examples of direct encapsulation of OLED using SALD systems discussed above, examples of thin-film encapsulation of OLED using ordinary ALD tools (temporal, cross-flow) are numerous, the first one being published in 2003 [145]. One example of SALD used to deposit a barrier layer onto an OLED device has been presented recently by Choi et al. [71]: the authors present a 'newly developed' reactor capable of processing Gen 2 substrates (370 × 470 mm^2, Fig. 15).

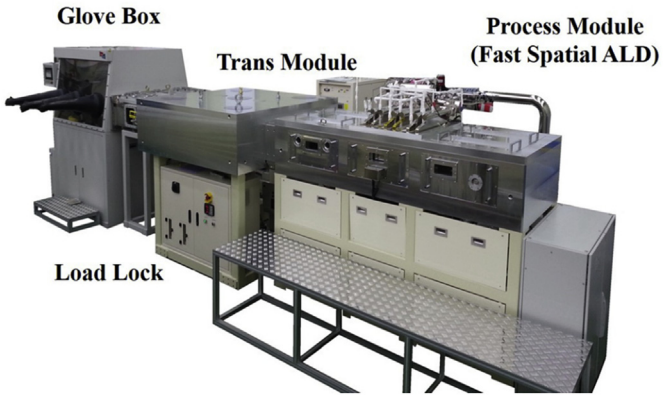

Fig. 15. Photograph of the fast spatial ALD system used by Choi et al. to encapsulate OLED panels reproduced with permission from Ref. [71]. ALD, atomic layer deposition; OLED, organic light-emitting diode.

The size of substrates used in the display industry can be up to Gen 10, that is, to say ~2.9 × 3.1 m^2 glass panels. This highlights one of the main requirements for ALD and SALD: the scale up to such large size substrates is mandatory, ensuring the same quality for the barrier layers at each generation while keeping cost low and HT. The advantage of the reactor developed by Choi et al. is an ALD deposition made with very short cycle times, i.e. below the second per cycle, at low temperature (typically <100 °C). In the end, the authors of this work show that it is possible to realize an Al_2O_3 barrier film of excellent quality for the encapsulation of OLED with a WVTR <3 × 10^{-3} g/m^2/day, resulting in a long lifetime for the OLED, compared with the non-encapsulated reference device (Fig. 16).

Another example of encapsulation of thin-film optoelectronics devices concerns the integration of an active impermeable electron extraction layer in a perovskite solar cell. This kind of thin-film devices resemble OLED very much in the sense that they use organic semiconductors as charge transport layers. In the end, they are at least as sensitive to moisture as their OLED counterparts [152]. The photoactive material is however of a different nature compared with OLEDs, being an inorganic perovskite or hybrid inorganic-organic perovskite. LED devices based on perovskite technology will probably in the future require the same level of barrier quality as for OLED [79]. Hoffman et al. proposed to use a SnO_2, deposited by SALD from Tetrakis(dimethylamino)tin(IV) (TDMASn) and H_2O as an extraction layer for electrons in a perovskite-based photovoltaic device. They claim that by doing this the barrier against atmosphere is 'embedded' inside the device itself. Interestingly, the authors observed a difference in the lifetime

Table 2
List of recent works that published WVTR measurements for oxide barrier layers deposited by SALD onto plastic foils.

Reference	Reactor type	Deposition speed	Substrate nature	WVTR (g/m^2/day)
[66]	Continuous ALD system (Beneq TFS 200R)	1.66 nm/min	Paper/polypropylene/Al_2O3 (100 nm)	7 × 10^{-1} (23 °C/50% RH)
	Batch ALD (Beneq TFS 500)	0.33 nm/min	Paper/polypropylene/Al_2O_3 (100 nm)	3 × 10^{-1} (23 °C/50% RH)
[52]	R2R-SALD	–	PET/Al_2O_3 (15–40 nm)	6 × 10^{-3} (37.8 °C/100% RH)
[51]	R2R-SALD	180 m^2/day	PEN/Al_2O_3 (20 nm)	<5 × 10^{-4} (38 °C/90% RH)
[73]	SALD (Beneq TFS 200R)	–	PEN/Al_2O_3 (20 nm)	<5 × 10^{-5} (38 °C/90% RH)
[69]	SALD (Plasma, Sentech)	2.3 nm/min	Glass/calcium/Al_2O_3 (50 nm)	4 × 10^{-6} (25 °C/50% RH)
[150]	SALD (plasma, Sentech)	–	Glass/calcium/Al_2O_3 (100 nm)	7 × 10^{-4} (60 °C/60% RH)
[151]	SALD (Beneq TFS 200R)	–	PEN/TiO_2 (20 nm)	5 × 10^{-4} (38 °C/90% RH)
[70]	R2R-SALD (for Al_2O_3 only)	0.9 nm/pass	PET/Al_2O_3 (30 nm)/PVA/Al_2O_3 (30 nm)/PVA	2.3 × 10^{-2} (37.8 °C/100% RH)
[68]	SALD (plasma, O_3, H_2O)	–	Glass/calcium/SnO_2 (110 nm)	7 × 10^{-4} (60 °C/60% RH)

WVTR, water vapor transmission rate; ALD, atomic layer deposition; SALD, spatial ALD; R2R, roll-to-roll; PEN, polyethylene naphthalate (poly(ethylene 2,6-naphthalate); PET, polyethylene terephthalate; PVA, polyvinyl alcohol; RH, relative humidity.

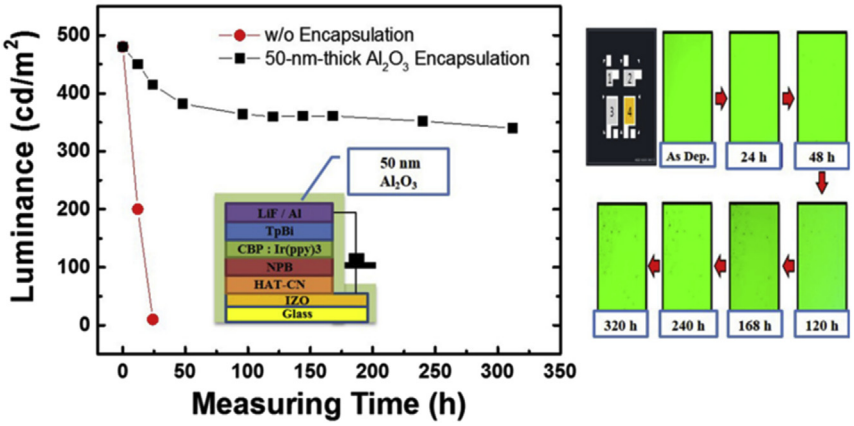

Fig. 16. Emission lifetime evaluation of Al_2O_3 encapsulation on an OLED panel reproduced with permission from Ref. [71]. OLED, organic light-emitting diode.

of the device, at laboratory ambient, vs. the substrate velocity in the SALD reactor (Fig. 17).

Substrate velocity in SALD systems in particular or precursor wave speed in fast temporal reactors will probably play a major role onto the barrier properties. By extrapolation, it is wise to think that high-speed deposition in real ALD mode in fast reactors could also have an impact on the doping efficiency of binary compounds. As discussed above, modeling of the reactors and processes (both chemical and fluid dynamic) will play a major role in obtaining high-quality barriers at HT.

5.2. HT ALD onto top-emitting OLED developed at CEA-LETI

The OLED research group at CEA-LETI has been working on ALD for OLED microdisplay thin-film encapsulation since 2006. The first generation of ALD systems was composed of R&D tools like the Savanah 200 system. In 2015, the group acquired an Infinity 200 tool from the French company Encapsulix. This tool was designed for 200 mm diameter substrates, silicon, or glass wafers. The mainstream process in the tool is Al_2O_3 from TMA/H_2O. Very short ALD cycle times of 3 s have been optimized at 90 °C, so as to preserve the OLED integrity. A dedicated attention has been paid so as to manage the level of particle contamination inside the reactor so as to provide pinhole-free barrier layers, as thin as 25 nm thick. The typical characteristics of the Al_2O_3 made in this fast PPWR reactor (see the description of the technology above for details) have been detailed in Fig. 18.

As a result, an optimized process has led to the realization of high quality Al_2O_3 barrier films and the obtained single Al_2O_3-encapsulated OLEDs can live several months in the laboratory atmosphere, without any noticeable degradation (Fig. 19).

More details of the OLED top-emitting structure we have developed at CEA-LETI can be found for instance in Ref. [153]. The interesting point in these structures lies in their emitting

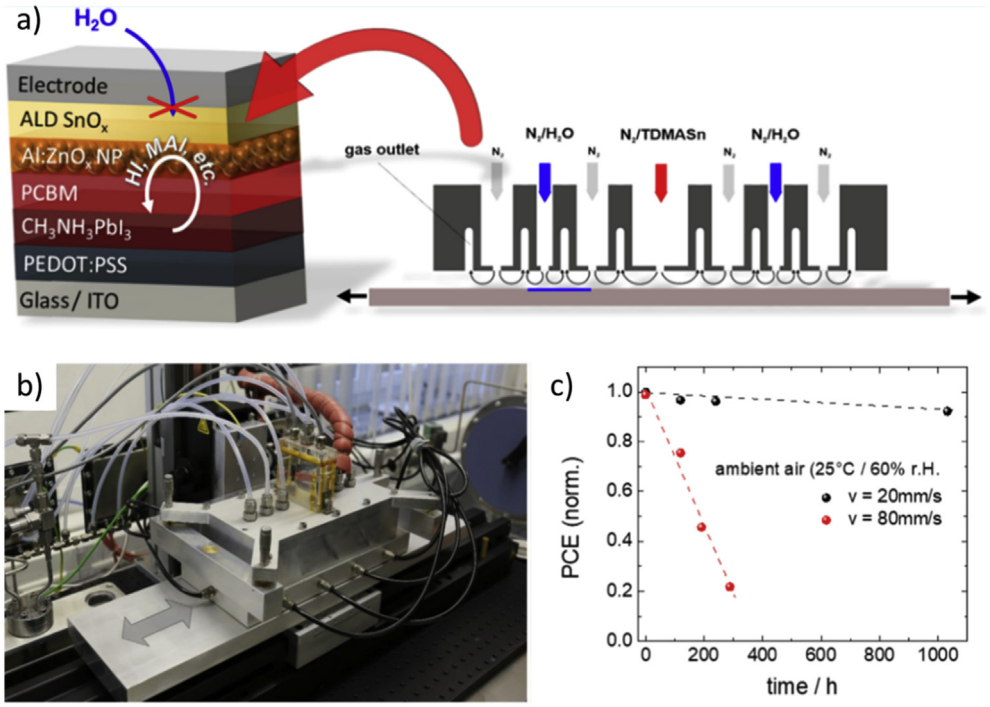

Fig. 17. (a) Schematic of the SALD assembly used to deposit a SnO_x layer as part of a perovskite solar cell stack [79]; (b) plasma SALD system inside a globe box for the deposition of SnO_x layers for solar cells based on hybrid perovskites; (c) normalized photoconversion efficiency (PCE) vs. time of storage in ambient air (25 °C, 60% RH) for solar cells with SALD SnO_x layers grown at 20 and 80 mm/s, respectively. (Images courtesy of Prof. T. Riedl). SALD, spatial ALD; ALD, atomic layer deposition.

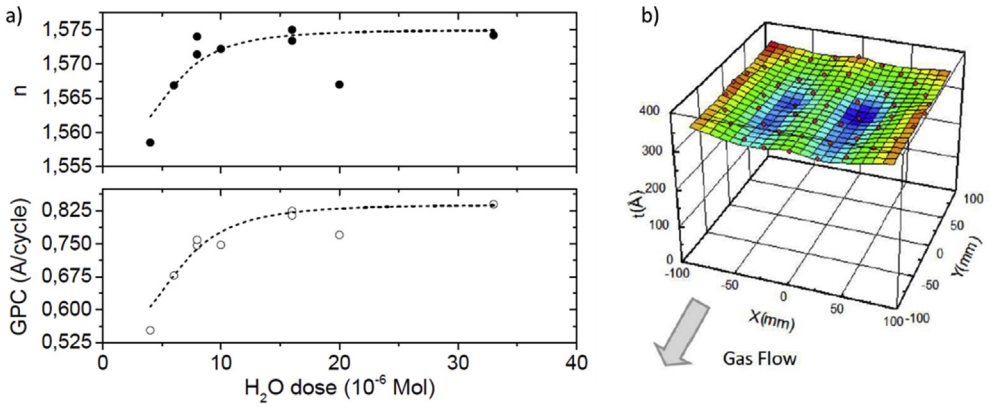

Fig. 18. 25 nm thick Al_2O_3 film made in a PPWR Infinity 200 reactor, 3 s/cycle, 90 °C. (a) optical index (n) and GPC vs. the H_2O dose; (b) non-uniformity of the alumina layer measured on a 200 mm Si wafer. Source: CEA-LETI. GPC, growth per cycle.

configuration. The light emitted inside the OLED under forward bias is extracted out from the top of the structure, which corresponds to the side where the device has been encapsulated with the Al_2O_3 barrier film. Such Al_2O_3 films, and a fortiori those made using the fast ALD from Encapsulix, are highly suitable in this configuration because their optical transmission is very high in the visible so that light absorption is minimized (in fine negligible compared with the absorbed light in the metallic, semi-transparent Ag electrode, through which light is extracted out).

5.3. Other materials of interest for the construction of barrier layers by HT ALD

Apart from the most used Al_2O_3 material in ALD technology for thin-film encapsulation, alternative metal oxides can be a priori good candidates for low-temperature ALD encapsulation, if one considers that the premium quality of ALD-deposited films, their pinhole-free characteristics constitutes the main prerequisite to ensure a very low WVTR. Among these alternative materials, ZnO, ZnO: Al (AZO), rapid SiO_2, TiO_2, Ta_2O_5, HfO_2, or SnO_2 could be cited. Barrier properties of rapid SiO_2 by ALD are close to the ones obtained with conventional deposition methods for rapid SiO_2. Compared with Al_2O_3 made by ALD, its main advantage is the high GPC, i.e. 12 nm/cycle, as described in Ref. [148]. The deposition mode was however made in a semi-static mode (reactor is soaked with a given precursor by closing the gate valve in the pumping line), which leads to long deposition run of 15 min/cycle, for a total number of five cycles, leading to 75 min deposition for the 60 nm thick SiO_2. This procedure has been adopted probably because of the low reactivity of the SiO_2 precursor, tris(tert-pentoxy)silanol. In the end, very nice results employing the bilayer [Al_2O_3/rapid SiO_2] were obtained, with WVTR as low as 1×10^{-4} g/m^2/day. In the end, the integration of such precursors into HT ALD systems might be tricky in the sense that HT ALD tools need precursors that react fast and efficiently.

'How fast ALD tools can go' is intrinsically related to the material to be processed, from a given couple precursor/oxidant. If one uses fast deposition material together with a HT ALD tool, the winning combination would be obtained. The case of SnO_2 as well as TiO_2 as barrier films is interesting. The recent publication from Behrendt et al. has shown that SnO_2 deposited by ALD from TDMASn and H_2O_2 or O_2 plasma had a low WVTR value while maintaining a high stability in a moisturized environment, at least compared with ALD-deposited Al_2O_3 in the same conditions (low temperature) [154]. Fig. 20a shows the evolution of the conductivity of different films deposited by ALD (standard cross-flow in that case, not fast ALD). It can be seen that the conductivity of SnO_2 remains very stable compared with ZnO or AZO material deposited in the same conditions. The authors concluded that his material is more stable under humidity ingress compared to ZnO and AZO. The study was performed under 85 °C/85% RH storage conditions.

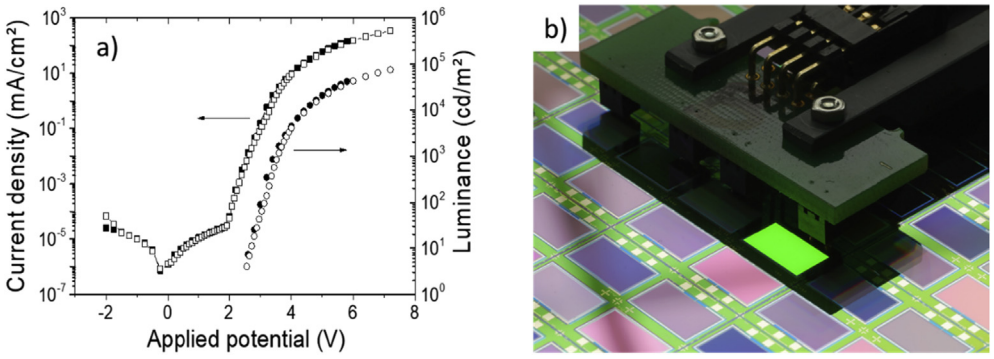

Fig. 19. (a) IVL characteristics of a green top-emitting OLED encapsulated with a single 25 nm-thick Al_2O_3 barrier layer deposited by HT ALD (3 s/cycle, 90 °C, TMA/H_2O) in an Infinity 200 tool from Encapsulix—initial time, freshly-made device (filled symbols), and after 22 months in laboratory atmosphere (open symbols); (b) picture of the green-emitting OLED surface under 3.2 V forward bias, after 22 months (no dark spots, similar quality as freshly-made device). Source: CEA-LETI. OLED, organic light-emitting diode; HT, high-throughput; ALD, atomic layer deposition; TMA, trimethylaluminum.

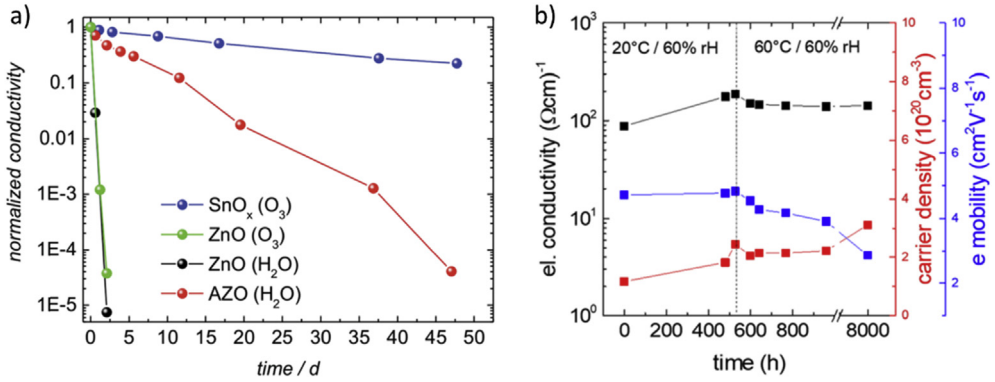

Fig. 20. (a) Normalized conductivity upon aging under damp heat conditions (85 °C and 85% RH) of 200 nm thick ZnO, AZO, and SnO_x films (grown at 150 °C) using O_3 or H_2O as oxidants; (b) electrical conductivity, carrier density, and electron mobility of SnO_2 deposited by HT PE-ALD. Reproduced with permission from Ref. [154]. ALD, atomic layer deposition; HT, high-throughput.

More recently, Hoffman et al. have shown that SnO_2 from TDMASn/O_2 plasma can be deposited by HT PE-ALD (Table 2). A very attractive WVTR of 7×10^{-4} g/m^2/day (at 60 °C/60% RH) has been obtained for 110 nm-thick SnO_2 films as well as a very interesting reliability study based on the monitoring of the electrical conductivity up to 8000 h (Fig. 20b), which showed almost no increase (from 10^{+2} (ohm.cm)$^{-1}$ at initial time up to only $2 \times 10^{+2}$ (ohm.cm)$^{-1}$) [68]. The high reliability under moisture and low WVTR of SnO_2 ALD films, by standard and fast ALD, makes this material a serious candidate for making atmospheric barrier films.

In the same manner, TiO_2 deposited by standard ALD has been claimed to be robust to moisture [155]. It has been recently deposited by SALD, see Table 2, onto PEN films [151]. Good WVTR of 5×10^{-4} g/m^2/day (at 38 °C/90% RH) have been measured for 20 nm-thick films. R2R ALD of TiO_2 has been performed by the LOTUS Applied Technology company [44]. Despite a good barrier quality, authors discussed the issue related to particle contamination issuing from movement of plastic films in the R2R system: the ALD coating on particles and bumps in the substrate surface rubs against the adjacent web in the take-up coil (rewind process in the full R2R process, unwind + rewind − band mode means that no rewind is made, only unwind). The thin ALD coating may then be cracked or debris may be displaced resulting in point defects in the barrier. The effect on the permeation performance can be critical, as shown in Fig. 21.

As shown in the plot, for thin ALD films, the WVTR of films processed in R2R mode is generally higher than that of films processed in the band mode. For thicker films, the WVTR of the R2R films plateaus in the low 10^{-3} g/m^2/day range and does not improve with increasing thickness. Generation of particles due to the substrate movement must thus be taken into account when designing a SALD system.

TiO_2 films have been made at CEA-LETI as thin-film encapsulation for OLED. The principal characteristics of the TiO_2 films have been summarized in Table 3, together with the ones for Al_2O_3 made in the same reactor, at the same temperature (90 °C).

The main result is that the TiO_2 process can be implemented onto an OLED without affecting its characteristics. The process is still under development and work has to be done to improve in particular the non-uniformity of the TiO_2 process.

5.4. (HT) Molecular layer deposition

The ALD growth mode can be used for the growth of organic polymers. This growth of polymer films is named MLD, which stands for molecular layer deposition. According to the same principle as for ALD, a molecular fragment is deposited during each cycle of MLD. Recently, many studies have shown film deposition by standard MLD to produce thin hybrid [MLD/ALD/ …] films with excellent mechanical stability and flexibility [156] compared with pure inorganic barrier films deposited by ALD. This strategy is somehow similar to multilayer stacks of the kind [Al_2O_3/polymer/ …] made by a dedicated PVD process that were implemented onto plastic films or OLED so as to achieve very low WVTR down to 10^{-6} g/m^2/day [157]. The production of these hybrid multilayers in the same ALD deposition chamber makes it possible to minimize the impact of defects added during transfers between deposition

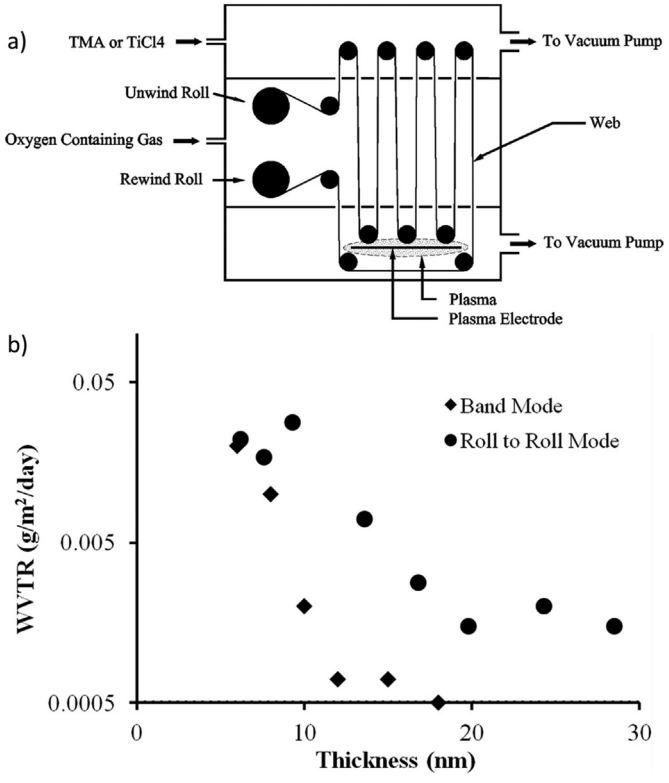

Fig. 21. (a) Schematic representation of the LOTUS applied technology roll-to-roll (R2R) reactor configured for plasma-based SALD; (b) Chart of water vapor barrier performance for ALD TiO_2 films on 'generic' industrial grade PET, deposited by substrate translation. Reproduced with permission from Ref. [44]. ALD, atomic layer deposition; SALD, spatial ALD; WVTR, water vapor transmission rate; TMA, trimethylaluminum.

Table 3
Main characteristics of Al_2O_3 and TiO_2 made in an Infinity 200 system at CEA-LETI, from TMA/H_2O and TTIP/H_2O, respectively, at 90 °C, onto 200 mm Si wafers. Efficiency (lumen per watt) of top-emitting green OLED using each material have been added.

Material	GPC (Å/cycle)	Time per cycle (s)	Non-uniformity (1 sigma)	Optical index n at 633 nm (30 nm)	OLED efficiency (lm/w)
Al_2O_3	0.85	<3	2.5	1.57	32.6
TiO_2	0.28	<3	5.7	2.10	31.2

GPC, growth per cycle; TMA, trimethylaluminum; OLED, organic light-emitting diode; TTIP, titanium isopropoxide.

machines. Usually, these MLD produces films that are called metalcone. They are made using standard organometallic precursors, as for instance TMA, oxidized by an alcohol, in that case leading to Alu(cone).

WVTR values of hybrid [Al_2O_3/alucone/ …] films were measured at ~ 2×10^{-2} g/m^2/day, which turns out to be better than WVTRs of single Al_2O_3 or alucone made under the same conditions, respectively 3.7×10^{-2} g/m^2/day and 1.14 g/m^2 day [158]. Since the alucone (or metalcone in general) film is partially organic, its WVTR is very high as organic phases are porous to water (and oxygen). Their role in hybrid [MLD/ALD/…] is therefore only to provide a decoupling effect between inorganic ALD layer defects and to contribute to an enhanced mechanical stability.

A very recent article showed the realization of a fast MLD process of polyamide films using sequential exposures of trimesoyl chloride and *m*-phenylenediamine. Using a SALD system, authors claimed polymer growth rate >1900 Å/min at a rotation speed of 210 RPM [67]. Another group has recently proposed to make a hybrid (PVA/Al_2O_3 [R2R-SALD]) (Table 2) [70]. In that case, however, the PVA polymer was done using a spray derivative technique, not MLD, but taking advantage of the open air processing offered by SALD to combine it with other atmospheric deposition techniques in a sequential (or in-line) mode (Fig. 22).

The performance of the hybrid has been measured in terms of WVTR, showing a low value down to 2.3×10^{-2} g/m^2/day. Combining both technologies, e.g. polyamide fast MLD + Al_2O_3 fast ALD could pave the way to the development of HT hybrid processes.

6. Outlook/perspectives

Table 4 below gives an overview of processing times and target cost for different industries that make use of thin-film materials, processed by vacuum deposition technologies. Except for the food packaging industry, where thicknesses of materials are usually too high for the ALD technology, ALD, if fast enough, will probably penetrate in a while some markets other than the microelectronics one.

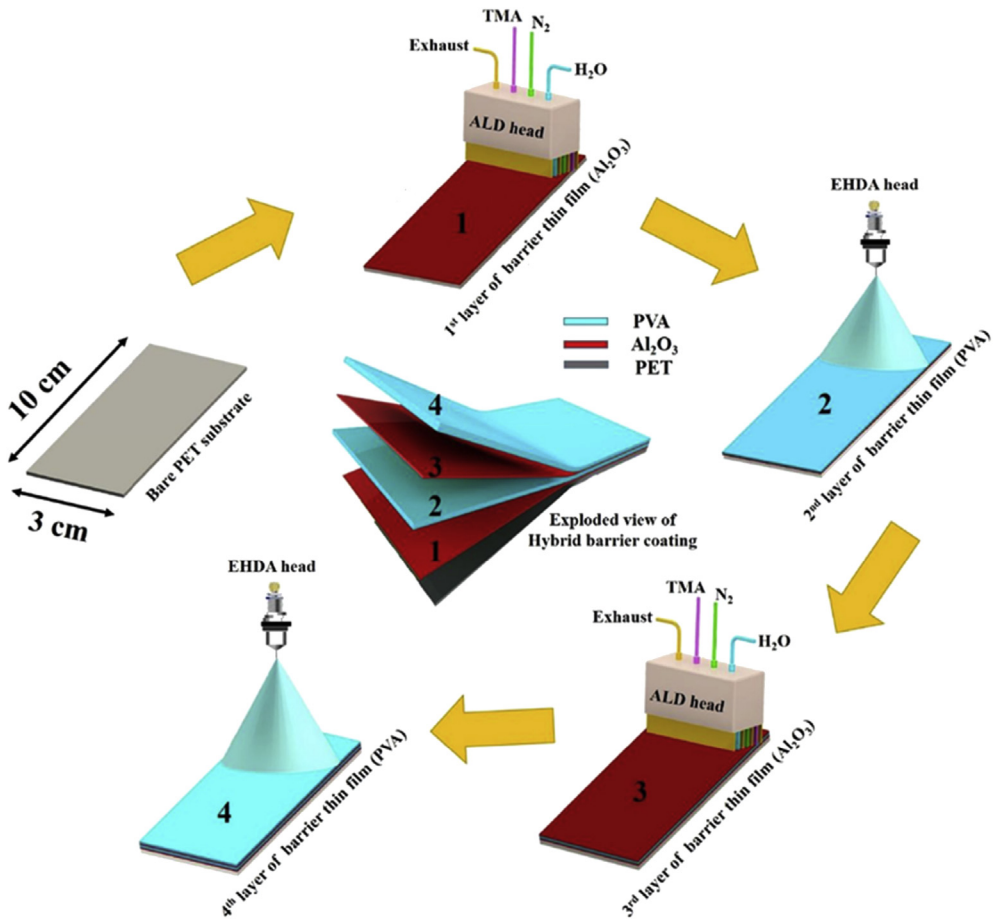

Fig. 22. Flow process diagram of hybrid multilayer barrier coating containing bare PET substrate reproduced with permission from Ref. [70]. ALD, atomic layer deposition; TMA, trimethylaluminum; EHDA, electrohydrodynamic atomization.

Table 4
Processing times and target cost for different industries that make use of thin-film materials.

Deposition technology	Typical target thickness (nm)	Typical deposition rate (nm/s)	Processing time (s)	Target cost (k€/m^2)
Packaging industry, PVD (large area)	50–500 [134]	10	50	0.0001
Microelectronics, PVD (TBD)	100	1	100	350
Microelectronics, ALD (HfO_2, Al_2O_3, 200–300 mm wafers)	2	0.015	133	
TFE for display industry, ALD (x-flow, low temp, Al_2O_3, 200 × 200 mm^2 substrates)	50	0.003	16666	5
TFE for display, ALD (PPW, low temp, Al_2O_3, 200 × 200 mm^2 substrates)	50	0.02[a]	2500	

PPW, parallel precursor wave; ALD, atomic layer deposition; OLED, organic light-emitting diode; TFE, thin film encapsulation.
[a] Assuming CEA-LETI process conditions onto OLED (25 nm in 20 min roughly).

The different approaches to HT discussed above have shown high deposition rates while being capable of retaining the high conformality and quality of conventional ALD films. As a consequence, we should expect to see ALD implemented industrially in an increasing number of applications and fields, such as these detailed in Table 4. From the different results and reports published from studies performed at the lab scale, it seems that HT ALD should result very attractive for device encapsulation and for device optimization through interface and surface nanoengineering. In particular, SALD has been widely used in the context of optoelectronic devices [29,159] for the deposition of diverse components such as blocking layers [37,38], transparent electrodes [160–166], interface layers [33,74,167], charge extraction layers in LED [61,168], and encapsulation layers [79]. The first industrial application of SALD has indeed been the deposition of Al_2O_3 passivation layers on crystalline Si solar cells. Therefore, in the coming years, HT ALD should undergo a significant industrial penetration in the field of optoelectronic devices.

The widespread utilization of HT ALD is going nevertheless to depend on different factors. First, most HT ALD approaches and processes depend on high-volatility, high-reactivity precursors. So, if materials other than Al_2O_3 and ZnO based ones are to be industrially implemented, new chemistry would have to be developed to widen the panoply of materials that can be deposited by HT ALD. The same applies to organic and hybrid materials deposited by MLD, with encouraging initial results by spatial MLD, as discussed above [67]. Secondly, and as has been shown above, in some cases, the use of plasma activation can contribute to an increase in the deposition rate and film quality. While atmospheric plasma has already been implemented for the deposition of oxides and metals with SALD [68,143,150,169–171], scaling up to large substrates will remain a technical challenge. As for batch ALD, plasma activation can only be done with remote plasma solutions, thus limiting the chemistry that can be performed in such HT ALD reactors. In the same line, the coating of high-aspect-ratio features with PEALD is already a challenge in conventional ALD systems, and solutions and strategies such as substrate biasing are currently being explored [172]. The nature of the best solutions that will be developed will determine whether they can be easily transposed to HT ALD approaches such as SALD or implemented in the design of HT ALD reactors.

Finally, cutting-edge research in the ALD filed in the last years involve the development of area selective ALD deposition and atomic layer etching (ALE). An approach widely followed for the area selective deposition of ALD layers has been the preconditioning of the sample surface with patterned regions in which a growth inhibitor is deposited [173–175]. The possibility to have HT ALD and selective deposition will depend on the type of device to be fabricated. If for instance several patterning steps are required, an atmospheric HT ALD approach such as SALD would be the most favorable to minimize the overhead times. This will be so in the cases in which the patterning will not require nanometric resolutions. The group from Kodak has indeed already demonstrated that complex devices could be fabricated by SALD through selective area deposition [55–58]. For devices requiring nanopatterning, the throughput will be limited by the patterning steps. Another approach to selective deposition is the use of plasma to activate the surface selectively [176]. The group from TNO has shown that this approach can also be applied in SALD reactors [170].

ALE is a technique in which thin layers of material are removed from a surface following self-limiting sequential reaction steps, and therefore it can be regarded as a subtractive counterpart of ALD. ALE is of interest for the microelectronic industry as an alternative to continuous etching since it provides more control at the atomic level and therefore allows for more complex devices to be fabricated. While ALD has been used in industry for many years now, ALE is still not suitable for industrial application since cycle times are excessively long (i.e. minutes). A review has recently been published on ALE and its implementation in the microelectronic industry [177]. Efforts are being currently done to reduce the ALE cycles, including the combination of SALD with spatial plasma etching to have HT ALE and selective deposition [178].

7. Conclusions

Despite ALD has traditionally been regarded as an extremely low deposition technique, different approaches have succeeded in providing the unique assets of ALD, namely, high conformality, high film quality even at low temperature, and precise thickness control, at high deposition rates (few nm/s). These approaches include batch ALD, SALD, process engineering, and reactor design and optimization. With these approaches and for certain materials, ALD growth rates have equaled those obtained by CVD. In the case of SALD, the possibility to design open-air and atmospheric equipment also contributes to cost reduction, which is very important for applications in which cost must be orders of magnitude smaller than in microelectronics, the main application for which ALD has been used industrially. In all the HT ALD approaches, modeling plays a key role in optimizing the designs and understanding the fluid dynamics and reactions taking place for a particular process and reactor. Owing to the intrinsic complexity of HT ALD, modeling is to be done at different levels, going from DFT simulation of reactions to KMC simulations and fluid dynamic modeling.

At present, batch ALD is already used in the microelectronic industry and penetrates other markets, as for example, the protection of collector coins and the coloring of jewelry parts. Reactor design, an optimization has been applied to batch and conventional ALD systems and has also yielded new reactor concepts, such as the one proposed by Encapsulix, which are already being used in industry. Concerning process engineering, it can be readily implemented as it can be performed in conventional ALD systems. Finally, SALD is already used in industry, mainly to coat Si solar cells with an Al_2O_3 passivating layer. Taking into account the reports published in the last years, it seems that SALD should be more extensively used for the fabrication of components for

optoelectronic devices, including different types of solar cells and LEDs. SALD seems also an exceptional approach for the encapsulation of sensitive devices, such as OLED, and for the surface functionalization of materials, i.e. plastics. In this line, a new spin off from the Holst Center called SALDtech has just been created for the deposition of large-area encapsulation layers for the display industry.

There are new concepts such as area-selective deposition and atomic layer epitaxy that have received a lot of attention in the last years. The possibility to use PEALD to coat high-aspect-ratio features also depends on the development of new plasma processes, and it constitutes a highly active research field. In all these exciting fields, there is potential to achieve HT, as has been demonstrated for the area-selective deposition using SALD. But ultimately, the possibility to implement them with HT will depend on the solutions proposed in each case.

Declarations of interest

None declared.

Acknowledgments

D.M.R acknowledges funding through the Marie Curie Actions (FP7/2007–2013, Grant Agreement No. 631111) and the Agence Nationale de Recherche (ANR, France) via the project DESPATCH (No. ANR-16- CE05-0021). DMR also acknowledges funding from the European Union's Horizon 2020 FETOPEN-1-2016-2017 research and innovation programme under grant agreement 801464.

References

[1] F.J. Heiligtag, M. Niederberger, The fascinating world of nanoparticle research, Mater. Today 16 (2013) 262–271, https://doi.org/10.1016/j.mattod.2013.07.004.
[2] R.P. Feynman, There's plenty of room at the bottom, J. Microelectromech. Syst. 1 (1992) 60–66.
[3] C. Toumey, 35 atoms that changed the nanoworld, Nat. Nanotechnol. 5 (2010) 239. https://doi.org/10.1038/nnano.2010.61.
[4] B.D. Gates, Q. Xu, M. Stewart, D. Ryan, C.G. Willson, G.M. Whitesides, New approaches to Nanofabrication: molding, printing, and other techniques, Chem. Rev. 105 (2005) 1171–1196, https://doi.org/10.1021/cr030076o.
[5] W.A. Bryant, The fundamentals of chemical vapour deposition, J. Mater. Sci. 12 (1977) 1285–1306.
[6] T.S. Suntola, J. Antson, Method for producing compound thin films, 4,058, 1977, p. 430.
[7] B.R.L. Puurunen, Essay a short history of atomic layer Deposition: tuomo Suntola ' s atomic layer epitaxy, Chem. Vap. Depos. (2014) 332–344, https://doi.org/10.1002/cvde.201402012.
[8] E. Ahvenniemiandrew, R.A. Alimikhael, B. Berdovastefan, K. Han, K. Klibanovyury, K. Outi, I.K. Kuhsirina, A.R. Rauwelfred, R. Sajavaarahossein, S. Savinnathanaelle, E. Ahvenniemi, A.R. Akbashev, S. Ali, F.-M. Cedex, M. Berdova, D.C. Cameron, R. Chen, Review Article : Recommended Reading List of Early Publications on Atomic Layer Deposition — Outcome of the " Virtual Project on the History of ALD " Review Article : Recommended Reading List of Early Publications on Atomic Layer Deposition — Outcome of T, 010801, 2017, https://doi.org/10.1116/1.4971389.
[9] A. Devi, 'Old Chemistries' for new applications: perspectives for development of precursors for MOCVD and ALD applications, Coord. Chem. Rev. 257 (2013) 3332–3384, https://doi.org/10.1016/j.ccr.2013.07.025.
[10] E. Alvaro, A. Yanguas-gil, Characterizing the field of atomic layer Deposition : authors , topics , and collaborations, PLoS One 13 (2017) e0189137. Editor, https://doi.org/10.1371/journal. pone.0189137.
[11] T. Suntola, Atomic layer epitaxy, Thin Solid Films 216 (1992) 84–89, https://doi.org/10.1016/0040-6090(92)90874-B.
[12] S.M. George, Atomic layer deposition: an overview, Chem. Rev. 110 (2010) 111–131, https://doi.org/10.1021/cr900056b.
[13] M. Cassir, A. Ringuedé, L. Niinistö, Input of atomic layer deposition for solid oxide fuel cell applications, J. Mater. Chem. 20 (2010) 8987, https://doi.org/10.1039/c0jm00590h.
[14] J.R. Bakke, K.L. Pickrahn, T.P. Brennan, S.F. Bent, Nanoengineering and interfacial engineering of photovoltaics by atomic layer deposition, Nanoscale 3 (2011) 3482–3508, https://doi.org/10.1039/c1nr10349k.
[15] C. Marichy, M. Bechelany, N. Pinna, Atomic layer deposition of nanostructured materials for energy and environmental applications, Adv. Mater. 24 (2012) 1017–1032, https://doi.org/10.1002/adma.201104129.
[16] J. Lu, J.W. Elam, P.C. Stair, Synthesis and stabilization of supported metal catalysts by atomic layer deposition, Acc. Chem. Res. 46 (2013) 1806–1815, https://doi.org/10.1021/ar300229c.
[17] V. Miikkulainen, M. Leskelä, M. Ritala, R.L. Puurunen, Crystallinity of inorganic films grown by atomic layer deposition: overview and general trends, J. Appl. Phys. 113 (2013) 021301, https://doi.org/10.1063/1.4757907.
[18] S.A. Skoog, J.W. Elam, R.J. Narayan, Atomic layer deposition: medical and biological applications, Int. Mater. Rev. 58 (2013) 113–129, https://doi.org/10.1179/1743280412Y.0000000009.
[19] O. Graniel, M. Weber, S. Balme, P. Miele, M. Bechelany, Biosensors and Bioelectronics Atomic layer deposition for biosensing applications, Biosens. Bioelectron. 122 (2018) 147–159, https://doi.org/10.1016/j.bios.2018.09.038.
[20] M.T. Bohr, R.S. Chau, T. Ghani, K. Mistry, The high-k solution, IEEE Spectr 44 (2007) 29–35, https://doi.org/10.1109/MSPEC.2007.4337663.
[21] K. Cooper, Scalable nanomanufacturing-a review, Micromachines 8 (2017), https://doi.org/10.3390/mi8010020.
[22] K.P. Musselman, C.F. Uzoma, M.S. Miller, Nanomanufacturing: high-throughput, cost-effective deposition of atomic scale thin films via atmospheric pressure spatial atomic layer deposition, Chem. Mater. 28 (2016) 8443–8452, https://doi.org/10.1021/acs.chemmater.6b03077.
[23] E. Granneman, P. Fischer, D. Pierreux, H. Terhorst, P. Zagwijn, Batch ALD: characteristics, comparison with single wafer ALD, and examples, Surf. Coating. Technol. 201 (2007) 8899–8907, https://doi.org/10.1016/j.surfcoat.2007.05.009.
[24] G. Dingemans, B. Jongbloed, W. Knaepen, D. Pierreux, L. Jdira, H. Terhorst, Merits of batch ALD, ECS Trans. 64 (2014) 35–49.
[25] S.K. Chunduir, Passivating the p-side, Phot. Int. (2013) 90–111.
[26] Atomic Layer Deposition from Picosun: Shine and Surface Protection for Coins and Watches, AZO Mater. (2014). October 3, https://www.azom.com/article.aspx?ArticleID=11424. (Accessed 3 November 2018).
[27] T.S. Suntola, A.J. Pakkala, S.G. Lindfors, Apparatus for performing growth of compound thin films, 4,389, 1983, p. 973.
[28] D.H. Levy, D. Freeman, S.F. Nelson, P.J. Cowdery-Corvan, L.M. Irving, Stable ZnO thin film transistors by fast open air atomic layer deposition, Appl. Phys. Lett. 92 (2008) 192101, https://doi.org/10.1063/1.2924768.
[29] D. Muñoz-Rojas, J. MacManus-Driscoll, Spatial atmospheric atomic layer deposition: a new laboratory and industrial tool for low-cost photovoltaics, Mater. Horizons 1 (2014), https://doi.org/10.1039/c3mh00136a.
[30] R.L.Z. Hoye, S. Heffernan, Y. Ievskaya, A. Sadhanala, A.J. Flewitt, R.H. Friend, J.L. MacManus-Driscoll, K.P. Musselman, Engineering Schottky contacts in open-air fabricated heterojunction solar cells to enable high performance and ohmic charge transport, ACS Appl. Mater. Interfaces (2014), https://doi.org/10.1021/am5058663.
[31] K.P. Musselman, S. Albert-Seifried, R.L.Z. Hoye, A. Sadhanala, D. Muñoz-Rojas, J.L. MacManus-Driscoll, R.H. Friend, Improved exciton dissociation at semiconducting polymer:ZnO donor:acceptor interfaces via nitrogen doping of ZnO, Adv. Funct. Mater. 24 (2014), https://doi.org/10.1002/adfm.201303994. Accepted.
[32] B. Ehrler, K.P. Musselman, M.L. Böhm, F.S.F. Morgenstern, Y. Vaynzof, B.J. Walker, J.L. MacManus-Driscoll, N.C. Greenham, Preventing interfacial recombination in colloidal quantum dot solar cells by doping the metal oxide, ACS Nano 7 (2013) 4210–4220, https://doi.org/10.1021/nn400656n.
[33] C.L. Armstrong, M.B. Price, D. Muñoz-Rojas, N.J.K.L. Davis, M. Abdi-Jalebi, R.H. Friend, N.C. Greenham, J.L. MacManus-Driscoll, M.L. Böhm, K.P. Musselman, Influence of an inorganic interlayer on exciton separation in hybrid solar cells, ACS Nano 9 (2015) 11863–11871, https://doi.org/10.1021/acsnano.5b05934.
[34] N. Khare, M.Z. Ansari, R.L.Z. Hoye, D.C. Iza, J.L. MacManus-Driscoll, Elucidation of barrier homogeneity in ZnO/P3HT:PCBM junctions through temperature dependent I – V characteristics, J. Phys. D Appl. Phys. 49 (2016) 275302, https://doi.org/10.1088/0022-3727/49/27/275302.
[35] R.L.Z. Hoye, B. Ehrler, M.L. Böhm, D. Muñoz-Rojas, R.M. Altamimi, A.Y. Alyamani, Y. Vaynzof, A. Sadhanala, G. Ercolano, N.C. Greenham, R.H. Friend, J.L. MacManus-Driscoll, K.P. Musselman, Improved open- circuit voltage in ZnO-PbSe quantum dot solar cells by understanding and reducing losses arising from the ZnO conduction band tail, Adv. Energy Mater. 4 (2014), https://doi.org/10.1002/aenm.201301544 n/a-n/a.
[36] A.T. Marin, D. Muñoz-Rojas, D.C. Iza, T. Gershon, K.P. Musselman, J.L. MacManus-Driscoll, Novel atmospheric growth technique to improve both light absorption and charge collection in ZnO/Cu2O thin film solar cells, Adv. Funct. Mater. 23 (2013) 3413–3419, https://doi.org/10.1002/adfm.201203243.
[37] D. Muñoz-Rojas, H. Sun, D.C. Iza, J. Weickert, L. Chen, H. Wang, L. Schmidt-Mende, J.L. MacManus-Driscoll, High-speed atmospheric atomic layer deposition of ultra thin amorphous TiO 2 blocking layers at 100 °C for inverted bulk heterojunction solar cells, Prog. Photovoltaics Res. Appl. 21 (2013) 393–400, https://doi.org/10.1002/pip.2380.
[38] R.L.Z. Hoye, D. Muñoz-Rojas, D.C. Iza, K.P. Musselman, J.L. MacManus-Driscoll, High performance inverted bulk heterojunction solar cells by incorporation of dense, thin ZnO layers made using atmospheric atomic layer

deposition, Sol. Energy Mater. Sol. Cells 116 (2013) 197–202, https://doi.org/10.1016/j.solmat.2013.04.020.
[39] B. van S, D.J. Maas, A.S. Lexmond, C.I.M.A. Spee, A.E. Duisterwinkel, A.J.P.M. Vermeer, Apparatus and method for atomic layer deposition, EP 2159304 (A1), 2010.
[40] P. Poodt, A. Lankhorst, F. Roozeboom, K. Spee, D. Maas, A. Vermeer, High-speed spatial atomic-layer deposition of aluminum oxide layers for solar cell passivation, Adv. Mater. 22 (2010) 3564–3567, https://doi.org/10.1002/adma.201000766.
[41] D. Muñoz-Rojas, M. Jordan, C. Yeoh, A.T. Marin, A. Kursumovic, L. Dunlop, D.C. Iza, A. Chen, H. Wang, J.L. MacManus-driscoll, Growth of 5 cm2V − 1s − 1 mobility , p-type Copper (I) oxide (Cu2O) films by fast atmospheric atomic layer deposition (AALD) at 225 ° C and below, AIP Adv. 2 (2012) 042179, https://doi.org/10.1063/1.4771681.
[42] P. Poodt, D.C. Cameron, E. Dickey, S.M. George, V. Kuznetsov, G.N. Parsons, F. Roozeboom, G. Sundaram, A. Vermeer, Spatial atomic layer deposition: a route towards further industrialization of atomic layer deposition, J. Vac. Sci. Technol. A Vac. Surf. Film 30 (2012) 010802, https://doi.org/10.1116/1.3670745.
[43] K. Ali, K.-H. Choi, Low-temperature roll-to-roll atmospheric atomic layer deposition of Al2O3 thin films, Langmuir (2014), https://doi.org/10.1021/la503406v.
[44] E. Dickey, W.A. Barrow, High rate roll to roll atomic layer deposition, and its application to moisture barriers on polymer films, J. Vac. Sci. Technol. A Vac. Surf. Film 30 (2012) 021502, https://doi.org/10.1116/1.3678486.
[45] K. Ali, K.-H. Choi, N.M. Muhammad, Roll-to-Roll atmospheric atomic layer deposition of Al 2 O 3 thin films on PET substrates, Chem. Vap. Depos. (2014), https://doi.org/10.1002/cvde.201407126 n/a-n/a.
[46] P. Poodt, R. Knaapen, A. Illiberi, F. Roozeboom, A. van Asten, Low temperature and roll-to-roll spatial atomic layer deposition for flexible electronics, J. Vac. Sci. Technol. A Vac. Surf. Film 30 (2012) 01A142, https://doi.org/10.1116/1.3667113.
[47] K. Sharma, D. Routkevitch, N. Varaksa, S.M. George, Spatial atomic layer deposition on flexible porous substrates: ZnO on anodic aluminum oxide films and Al2O3 on Li ion battery electrodes, J. Vac. Sci. Technol. A Vac. Surf. Film 34 (2016) 01A146, https://doi.org/10.1116/1.4937728.
[48] K. Ali, J. Ali, S.M. Mehdi, K.-H. Choi, Y.J. An, Rapid fabrication of Al2O3 encapsulations for organic electronic devices, Appl. Surf. Sci. 353 (2015) 1186–1194, https://doi.org/10.1016/j.apsusc.2015.07.032.
[49] A.S. Yersak, Y.C. Lee, J.A. Spencer, M.D. Groner, Atmospheric pressure spatial atomic layer deposition web coating with in situ monitoring of film thickness, J. Vac. Sci. Technol. A Vac. Surf. Film 32 (2014) 01A130, https://doi.org/10.1116/1.4850176.
[50] K. Sharma, R.A. Hall, S.M. George, Spatial atomic layer deposition on flexible substrates using a modular rotating cylinder reactor, J. Vac. Sci. Technol. A Vac. Surf. Film 33 (2015) 01A132, https://doi.org/10.1116/1.4902086.
[51] P.S. Maydannik, T.O. Kääriäinen, K. Lahtinen, D.C. Cameron, M. Söderlund, P. Soininen, P. Johansson, J. Kuusipalo, L. Moro, X. Zeng, Roll-to-roll atomic layer deposition process for flexible electronics encapsulation applications, J. Vac. Sci. Technol. A 32 (2014) 51603, https://doi.org/10.1116/1.4893428.
[52] K. Ali, K.-H. Choi, J. Jo, Y.W. Lee, High rate roll-to-roll atmospheric atomic layer deposition of Al2O3 thin films towards gas diffusion barriers on polymers, Mater. Lett. 136 (2014) 90–94. https://doi.org/10.1016/j.matlet.2014.07.186.
[53] R.L.Z. Hoye, D. Muñoz-Rojas, S.F. Nelson, A. Illiberi, P. Poodt, F. Roozeboom, J.L. MacManus-Driscoll, Research Update: atmospheric pressure spatial atomic layer deposition of ZnO thin films: reactors, doping, and devices, APL Mater 3 (2015) 040701, https://doi.org/10.1063/1.4916525.
[54] D.H. Levy, S.F. Nelson, D. Freeman, Oxide electronics by spatial atomic layer deposition, J. Disp. Technol. 5 (2009) 484–494. http://jdt.osa.org/abstract.cfm?URI=jdt-5-12-484. (Accessed 27 June 2012).
[55] D.H. Levy, C.R. Ellinger, S.F. Nelson, Metal-oxide thin-film transistors patterned by printing, Appl. Phys. Lett. 103 (2013) 043505, https://doi.org/10.1063/1.4816322.
[56] C.R. Ellinger, S.F. Nelson, Selective area spatial atomic layer deposition of ZnO, Al 2 O 3 , and aluminum-doped ZnO using poly(vinyl pyrrolidone), Chem. Mater. 26 (2014) 1514–1522, https://doi.org/10.1021/cm402464z.
[57] S.F. Nelson, C.R. Ellinger, D.H. Levy, Improving yield and performance in ZnO thin-film transistors made using selective area deposition, ACS Appl. Mater. Interfaces 7 (2015) 2754–2759, https://doi.org/10.1021/am5077638.
[58] C.R. Ellinger, S.F. Nelson, Design freedom in multilayer thin-film devices, ACS Appl. Mater. Interfaces 7 (2015) 4675–4684, https://doi.org/10.1021/am508088p.
[59] M. Goe, G. Gaustad, Identifying critical materials for photovoltaics in the US : a multi-metric approach, Appl. Energy 123 (2014) 387–396, https://doi.org/10.1016/j.apenergy.2014.01.025.
[60] R.L.Z. Hoye, R.E. Brandt, Y. Ievskaya, S. Heffernan, K.P. Musselman, T. Buonassisi, J.L. MacManus-Driscoll, Perspective: maintaining surface-phase purity is key to efficient open air fabricated cuprous oxide solar cells, APL Mater. 3 (2015) 020901, https://doi.org/10.1063/1.4913442.
[61] R.L.Z. Hoye, M.R. Chua, K.P. Musselman, G. Li, M.-L. Lai, Z.-K. Tan, N.C. Greenham, J.L. MacManus-Driscoll, R.H. Friend, D. Credgington, Enhanced performance in fluorene-free organometal halide perovskite light-emitting diodes using tunable, low electron affinity oxide electron injectors, Adv. Mater. (2015), https://doi.org/10.1002/adma.201405044 n/a-n/a.
[62] D. Bellet, M. Lagrange, T. Sannicolo, S. Aghazadehchors, V.H. Nguyen, D.P. Langley, D. Muñoz-Rojas, C. Jiménez, Y. Bréchet, N.D. Nguyen, Transparent electrodes based on silver nanowire networks: from physical considerations towards device integration, Materials (Basel) 10 (2017) 570, https://doi.org/10.3390/ma10060570.
[63] T. Sannicolo, M. Lagrange, A. Cabos, C. Celle, J. Simonato, D. Bellet, Metallic nanowire-based transparent electrodes for next generation flexible Devices : a review, Small 12 (2016) 6052–6075, https://doi.org/10.1002/smll.201602581.
[64] C. Celle, A. Cabos, T. Fontecave, B. Laguitton, A. Benayad, L. Guettaz, N. Pélissier, V.H. Nguyen, D. Bellet, D. Muñoz-Rojas, J.-P. Simonato, Oxidation of copper nanowire based transparent electrodes in ambient conditions and their stabilization by encapsulation : application to transparent fi lm heaters, Nanotechnology 29 (2018) 085701.
[65] A. Khan, V.H. Nguyen, D. Muñoz-Rojas, S. Aghazadehchors, C. Jiménez, N.D. Nguyen, D. Bellet, Stability enhancement of silver nanowire networks with conformal ZnO coatings deposited by atmospheric pressure spatial atomic layer deposition, ACS Appl. Mater. Interfaces (2018), https://doi.org/10.1021/acsami.8b03079.
[66] K. Lahtinen, P. Maydannik, P. Johansson, T. Kääriäinen, D.C. Cameron, J. Kuusipalo, Utilisation of continuous atomic layer deposition process for barrier enhancement of extrusion-coated paper, Surf. Coating. Technol. 205 (2011) 3916–3922, https://doi.org/10.1016/j.surfcoat.2011.02.009.
[67] D.J. Higgs, J.W. Dumont, K. Sharma, S.M. George, Spatial molecular layer deposition of polyamide thin films on flexible polymer substrates using a rotating cylinder reactor, J. Vac. Sci. Technol. A Vac. Surf. Film 36 (2018) 01A117.
[68] L. Hoffmann, D. Theirich, D. Schlamm, T. Hasselmann, S. Pack, K.O. Brinkmann, D. Rogalla, S. Peters, A. Räupke, H. Gargouri, T. Riedl, Atmospheric pressure plasma enhanced spatial atomic layer deposition of SnOx as conductive gas diffusion barrier, J. Vac. Sci. Technol. A 36 (2018) 01A112, https://doi.org/10.1116/1.5006781.
[69] S. Franke, M. Baumkötter, C. Monka, S. Raabe, R. Caspary, H.-H. Johannes, W. Kowalsky, S. Beck, A. Pucci, H. Gargouri, Alumina films as gas barrier layers grown by spatial atomic layer deposition with trimethylaluminum and different oxygen sources, J. Vac. Sci. Technol. A Vac. Surf. Film 35 (2017) 01B117, https://doi.org/10.1116/1.4971173.
[70] M. Mutee ur Rehman, K.T. Kim, K.H. Na, K.H. Choi, Atmospheric deposition process for enhanced hybrid organic- inorganic multilayer barrier thin films for surface protection, Appl. Surf. Sci. 422 (2017) 273–282, https://doi.org/10.1016/j.apsusc.2017.05.261.
[71] H. Choi, S. Shin, H. Jeon, Y. Choi, J. Kim, S. Kim, S.C. Chung, K. Oh, Fast spatial atomic layer deposition of Al2O3 at low temperature (<100 °C) as a gas permeation barrier for flexible organic light-emitting diode displays, J. Vac. Sci. Technol. A Vac. Surf. Film 34 (2016) 01A121, https://doi.org/10.1116/1.4934752.
[72] S.-Y. Lien, C.-H. Yang, K.-C. Wu, C.-Y. Kung, Investigation on the passivated Si/Al2O3 interface fabricated by non-vacuum spatial atomic layer deposition system, Nanoscale Res. Lett. 10 (2015) 93, https://doi.org/10.1186/s11671-015-0803-9.
[73] P.S. Maydannik, A. Plyushch, M. Sillanpää, D.C. Cameron, D.C. Cameron, Spatial atomic layer deposition : performance of low temperature H2O and O3 oxidant chemistry for flexible electronics encapsulation Spatial atomic layer deposition : performance of low temperature H 2 O and O 3 oxidant chemistry for flexible electronics, J. Vac. Sci. Technol. A 33 (2015) 031603, https://doi.org/10.1116/1.4914079.
[74] K.P. Musselman, D. Muñoz-Rojas, R.L.Z. Hoye, H. Sun, S.-L. Sahonta, E. Croft, M.L. Böhm, C. Ducati, J.L. MacManus-Driscoll, S. De Gendt, M. Heyns, M.M. Viitanen, M. de Ridder, H.H. Brongersma, Y. de Tamminga, T. Dao, T. de Win, M. Verheijen, M. Kaiser, M. Tuominen, Rapid open-air deposition of uniform, nanoscale, functional coatings on nanorod arrays, Nanoscale Horizon 2 (2017) 110–117, https://doi.org/10.1039/C6NH00197A.
[75] P. Poodt, A. Mameli, J. Schulpen, W.M.M.E.K. Roozeboom, F. Roozeboom, Effect of reactor pressure on the conformal coating inside porous substrates by atomic layer deposition, J. Vac. Sci. Technol. A (2017) 021502, https://doi.org/10.1116/1.4973350.
[76] A.S. Yersak, K. Sharma, J.M. Wallas, A.A. Dameron, X. Li, Y. Yang, K.E. Hurst, C. Ban, R.C. Tenent, S.M. George, A.S. Yersak, K. Sharma, J.M. Wallas, A.A. Dameron, Spatial atomic layer deposition for coating flexible porous Li-ion battery electrodes Spatial atomic layer deposition for coating flexible porous Li-ion battery electrodes, J. Vac. Sci. Technol. A 36 (2018) 01A123, https://doi.org/10.1116/1.5006670.
[77] S. Moitzheim, J.E. Balder, P. Poodt, S. Unnikrishnan, S. De Gendt, P.M. Vereecken, Chlorine doping of amorphous TiO 2 for increased capacity and faster Li + -ion storage, Chem. Mater. (2017), https://doi.org/10.1021/acs.chemmater.7b03478 acs.chemmater.7b03478.
[78] J.R. van Ommen, D. Kooijman, M. de Niet, M. Talebi, A. Goulas, Continuous production of nanostructured particles using spatial atomic layer deposition, J. Vac. Sci. Technol. A Vac. Surf. Film 33 (2015) 021513, https://doi.org/10.1116/1.4905725.
[79] L. Hoffmann, K.O. Brinkmann, J. Malerczyk, D. Rogalla, T. Becker, D. Theirich, I. Shutsko, P. Görrn, T. Riedl, Spatial atmospheric pressure atomic layer deposition of tin oxide as an impermeable electron extraction layer for perovskite solar cells with enhanced thermal stability, ACS Appl. Mater. Interfaces 10 (2018) 6006–6013, https://doi.org/10.1021/acsami.7b17701.

[80] V.H. Nguyen, U. Gottlieb, A. Valla, D. Muñoz, D. Bellet, D. Muñoz-Rojas, Electron tunneling through grain boundaries in transparent conductive oxides and implications for electrical conductivity: the case of ZnO:Al thin films, Mater. Horizons 5 (2018) 715–726, https://doi.org/10.1039/C8MH00402A.
[81] G. Biswas, M. Breuer, F. Durst, Backward-facing step flows for various expansion ratios at low and moderate Reynolds numbers, Trans. ASME 126 (2004) 362, https://doi.org/10.1115/1.1760532.
[82] J.C.S. Kools, R. Bubber, M. Mao, T. Schneider, J. Wang, Method and Apparatus for Fabricating a Conformal Thin Film on a Substrate, US7071118B2, 2005.
[83] V.H. Grassian, Surface science of complex environmental interfaces: oxide and carbonate surfaces in dynamic equilibrium with water vapor, Surf. Sci. 602 (2008) 2955–2962, https://doi.org/10.1016/j.susc.2008.07.039.
[84] J.C.S. Kools, Gas Injection Device with Uniform Gas Velocity, US 8721835, 2014, https://doi.org/10.1016/j.(73).
[85] M.D. Groner, F.H. Fabreguette, J.W. Elam, S.M. George, Low-temperature Al2O3 atomic layer deposition, Chem. Mater. 16 (2004) 639–645, https://doi.org/10.1021/cm0304546.
[86] T. Suntola, S. Lindfors, Method for Growing Thin Films, US7404984B2, 2008, https://doi.org/10.1145/634067.634234.
[87] S. Krumdieck, Pulsed-pressure MOCVD science, materials and technology, ECS Trans. (2009), https://doi.org/10.1149/1.3207726.
[88] F. Piallat, J. Vitiello, At the edge between metal organic chemical vapor deposition and atomic layer deposition: fast Atomic Sequential Technique, for high throughput conformal deposition, J. Vac. Sci. Technol. B Nanotechnol. Microelectron. Mater. Process. Meas. Phenom. 34 (2016) 021202, https://doi.org/10.1116/1.4942497.
[89] T. Kääriäinen, D. Cameron, M. Kääriäinen, A. Sherman, Fundamentals of atomic layer deposition, in: At. Layer Depos, 2013, https://doi.org/10.1002/9781118747407.ch1.
[90] R.F. B, Deposition technologies: an overview, P.M.B.T.-H. of D.T. for F. and C., in: Third E. Martin (Ed.), Handb. Depos. Technol. Film. Coatings, William Andrew Publishing, Boston, 2010, pp. 1–31 https://doi.org/10.1016/B978-0-8155-2031-3.00001-6.
[91] M. Leskelä, M. Ritala, Atomic layer deposition (ALD): from precursors to thin film structures, Thin Solid Films 409 (2002) 138–146, https://doi.org/10.1016/S0040-6090(02)00117-7.
[92] H.M. Cave, S.P. Krumdieck, M.C. Jermy, Development of a model for high precursor conversion efficiency pulsed-pressure chemical vapor deposition (PP-CVD) processing, Chem. Eng. J. 135 (2008) 120–128, https://doi.org/10.1016/j.cej.2007.03.027.
[93] D.J.H. Emslie, P. Chadha, J.S. Price, Metal ALD and pulsed CVD: fundamental reactions and links with solution chemistry, Coord. Chem. Rev. 257 (2013) 3282–3296, https://doi.org/10.1016/j.ccr.2013.07.010.
[94] J. Vitiello, F. Piallat, L. Bonnet, Alternative deposition solution for cost reduction of TSV integration, Int. Symp. Microelectron. (2017) (2017) 135–139, https://doi.org/10.4071/isom-2017-TP52_034.
[95] M. Gros-Jean, N. Jourdan, J. Michailos, Process and Device for Making a Tantalum Pentoxide Layer on a Carrier Material Particularly Titanium Nitride and Integreted Circuit Incorporating a Tantalum Pentoxide Layer, EP1427005A1, 2004.
[96] R.L.Z. Hoye, D. Muñoz-Rojas, K.P. Musselman, Y. Vaynzof, J.L. MacManus-Driscoll, Synthesis and modeling of uniform complex metal oxides by close-proximity atmospheric pressure chemical vapor deposition, ACS Appl. Mater. Interfaces (2015), https://doi.org/10.1021/am5073589, 150515102727002.
[97] L. Jeloaica, A. Esteve, M.D. Rouhani, D. Esteve, Density functional theory study of HfCl4, ZrCl4, and Al(CH3)(3) decomposition on hydroxylated SiO2: initial stage of high-k atomic layer deposition, Appl. Phys. Lett. 83 (2003) 542–544, https://doi.org/10.1063/1.1587261.
[98] S. Olivier, J.M. Ducere, C. Mastail, G. Landa, A. Esteve, M.D. Rouhani, Insights into crystalline preorganization of gas-phase precursors: densification mechanisms, Chem. Mater. 20 (2008) 1555–1560.
[99] S. Klejna, S.D. Elliott, First-Principles modeling of the “Clean-Up” of native oxides during atomic layer deposition onto III-V substrates, J. Phys. Chem. C 116 (2012) 643–654, https://doi.org/10.1021/jp206566y.
[100] S.D. Elliott, J.C. Greer, Simulating the atomic layer deposition of alumina from first principles, J. Mater. Chem. 14 (2004) 3246–3250, https://doi.org/10.1039/b405776g.
[101] S.D. Elliott, G. Dey, Y. Maimaiti, H. Ablat, E.A. Filatova, G.N. Fomengia, Modeling mechanism and growth reactions for new nanofabrication processes by atomic layer deposition, Adv. Mater 28 (2016) 5367–5380, https://doi.org/10.1002/adma.201504043.
[102] Y. Widjaja, C.B. Musgrave, Quantum chemical study of the elementary reactions in zirconium oxide atomic layer deposition, Appl. Phys. Lett. 81 (2002) 304–306, https://doi.org/10.1063/1.1490415.
[103] M. Shirazi, S.D. Elliott, Atomistic kinetic Monte Carlo study of atomic layer deposition derived from density functional theory, J. Comput. Chem. 35 (2014) 244–259, https://doi.org/10.1002/jcc.23491.
[104] G. Mazaleyrat, A. Esteve, L. Jeloaica, M. Djafari-Rouhani, A methodology for the kinetic Monte Carlo simulation of alumina atomic layer deposition onto silicon, Comput. Mater. Sci. 33 (2005) 74–82, https://doi.org/10.1016/j.commatsci.2004.12.069.
[105] A. Dkhissi, A. Esteve, C. Mastail, S. Olivier, G. Mazaleyrat, L. Jeloaica, M.D. Rouhani, Multiscale modeling of the atomic layer deposition of HfO2 thin film grown on silicon: how to deal with a kinetic Monte Carlo procedure, J. Chem. Theor. Comput. 4 (2008) 1915–1927, https://doi.org/10.1021/ct8001249.
[106] C.D. Travis, R.A. Adomaitis, Modeling alumina atomic layer deposition reaction kinetics during the trimethylaluminum exposure, Theor. Chem. Acc. 133 (2013) 1414, https://doi.org/10.1007/s00214-013-1414-0. UNSP 1414.
[107] E.M. Remmers, C.D. Travis, R.A. Adomaitis, Reaction factorization for the dynamic analysis of atomic layer deposition kinetics, Chem. Eng. Sci. 127 (2015) 374–391, https://doi.org/10.1016/j.ces.2015.01.051.
[108] M. Deminsky, A. Knizhnik, I. Belov, S. Umanskii, E. Rykova, A. Bagatur'yants, B. Potapkin, M. Stoker, A. Korkin, Mechanism and kinetics of thin zirconium and hafnium oxide film growth in an ALD reactor, Surf. Sci. 549 (2004) 67–86, https://doi.org/10.1016/j.susc.2003.10.056.
[109] R.L. Puurunen, Surface chemistry of atomic layer deposition: a case study for the trimethylaluminum/water process, J. Appl. Phys. 97 (2005) 121301, https://doi.org/10.1063/1.1940727.
[110] S. Shankar, H. Simka, M. Haverty, Density functional theory and beyond - opportunities for quantum methods in materials modeling semiconductor technology, J. Phys. Condens. Matter 20 (2008), https://doi.org/10.1088/0953-8984/20/6/064232. Artn 064232.
[111] M. Shirazi, S.D. Elliott, Cooperation between adsorbates accounts for the activation of atomic layer deposition reactions, Nanoscale 7 (2015) 6311–6318, https://doi.org/10.1039/c5nr00900f.
[112] T. Weckman, K. Laasonen, First principles study of the atomic layer deposition of alumina by TMA-H2O-process, Phys. Chem. Chem. Phys. 17 (2015) 17322–17334, https://doi.org/10.1039/c5cp01912e.
[113] A.S. Sandupatla, K. Alexopoulos, M.F. Reyniers, G.B. Marin, Ab initio investigation of surface chemistry of alumina ALD on hydroxylated gamma-alumina surface, J. Phys. Chem. C 119 (2015) 13050–13061, https://doi.org/10.1021/acs.jpcc.5b02382.
[114] C.D. Travis, R.A. Adomaitis, Modeling ALD surface reaction and process dynamics using absolute reaction rate theory, Chem. Vap. Depos. 19 (2013) 4–14, https://doi.org/10.1002/cvde.201206985.
[115] P. Poodt, J. van Lieshout, A. Illiberi, R. Knaapen, F. Roozeboom, A. van Asten, On the kinetics of spatial atomic layer deposition, J. Vac. Sci. Technol. A Vac. Surf. Film 31 (2013) 01A108, https://doi.org/10.1116/1.4756692.
[116] A. Holmqvist, T. Törndahl, S. Stenström, A model-based methodology for the analysis and design of atomic layer deposition processes—Part III: constrained multi-objective optimization, Chem. Eng. Sci. 96 (2013) 71–86, https://doi.org/10.1016/j.ces.2013.03.061.
[117] A. Holmqvist, T. Torndahl, S. Stenstrom, A model-based methodology for the analysis and design of atomic layer deposition processes-Part I: mechanistic modelling of continuous flow reactors, Chem. Eng. Sci. 81 (2012) 260–272, https://doi.org/10.1016/j.ces.2012.07.015.
[118] A. Holmqvist, T. Torndahl, S. Stenstrom, A model-based methodology for the analysis and design of atomic layer deposition processes-Part II: experimental validation and mechanistic analysis, Chem. Eng. Sci. 94 (2013) 316–329, https://doi.org/10.1016/j.ces.2012.06.063.
[119] J.C.S. Kools, High throughput atomic layer deposition for encapsulation of large area electronics, ECS Trans. 41 (2011) 195–201.
[120] A.M. Lankhorst, B.D. Paarhuis, H.J.C.M. Terhorst, P.J.P.M. Simons, C.R. Kleijn, Transient ALD simulations for a multi-wafer reactor with trenched wafers, Surf. Coat. Technol. 201 (2007) 8842–8848, https://doi.org/10.1016/j.surfcoat.2007.04.079.
[121] G.P. Gakis, H. Vergnes, E. Scheid, C. Vahlas, B. Caussat, A.G. Boudouvis, Computational Fluid Dynamics simulation of the ALD of alumina from TMA and H2O in a commercial reactor, Chem. Eng. Res. Des. 132 (2018) 795–811, https://doi.org/10.1016/j.cherd.2018.02.031.
[122] A. Yanguas-Gil, J.W. Elam, Simple model for atomic layer deposition precursor reaction and transport in a viscous-flow tubular reactor, J. Vac. Sci. Technol. A 30 (2012), https://doi.org/10.1116/1.3670396. Artn 01a159.
[123] Y.Y. Xie, L.L. Ma, D.Q. Pan, C. Yuan, Mechanistic modeling of atomic layer deposition of alumina process with detailed surface chemical kinetics, Chem. Eng. J. 259 (2015) 213–220, https://doi.org/10.1016/j.cej.2014.07.105.
[124] Z. Deng, W. He, C. Duan, R. Chen, B. Shan, Mechanistic modeling study on process optimization and precursor utilization with atmospheric spatial atomic layer deposition, J. Vac. Sci. Technol. A Vac. Surf. Film 34 (2016) 01A108, https://doi.org/10.1116/1.4932564.
[125] D. Pan, T.-C. Jen, C. Yuan, Effects of gap size, temperature and pumping pressure on the fluid dynamics and chemical kinetics of in-line spatial atomic layer deposition of Al2O3, Int. J. Heat Mass Transf. 96 (2016) 189–198, https://doi.org/10.1016/j.ijheatmasstransfer.2016.01.034.
[126] P.S. Maydannik, T.O. Kääriäinen, D.C. Cameron, An atomic layer deposition process for moving flexible substrates, Chem. Eng. J. 171 (2011) 345–349, https://doi.org/10.1016/j.cej.2011.03.097.
[127] P.S. Maydannik, T.O. Kaariainen, D.C. Cameron, Continuous atomic layer deposition: explanation for anomalous growth rate effects, J. Vac. Sci. Technol. A Vac. Surf. Film 30 (2012) 01A122, https://doi.org/10.1116/1.3662861.
[128] U.H. Frank, Transparent conductive oxides in thin film photovoltaics, J. Phys. Conf. Ser. 559 (2014) 12016. http://stacks.iop.org/1742-6596/559/i=1/a=012016.
[129] W. Cao, J. Li, H. Chen, J. Xue, Transparent electrodes for organic optoelectronic devices: a review, J. Photon. Energy 4 (2014) 040990, https://doi.org/10.1117/1.JPE.4.040990.

[130] T. Maindron, T. Jullien, A. André, Defect analysis in low temperature atomic layer deposited Al2O3 and physical vapor deposited SiO barrier films and combination of both to achieve high quality moisture barriers, J. Vac. Sci. Technol. A 34 (2016) 31513, https://doi.org/10.1116/1.4947289.
[131] Y. Lai, Z. Chen, Y. Huang, J. Zhang, The process and reliability tests of glass-to-glass laser bonding for top-emission OLED device, in: IEEE 62nd Electron. Components Technol. Conf., 2012, pp. 2036–2041.
[132] F. Templier, OLED Microdisplays: Technology and Applications, Wiley, Somerset, 2014.
[133] T. Hirvikorpi, M. Vähä-Nissi, A. Harlin, M. Karppinen, Comparison of some coating techniques to fabricate barrier layers on packaging materials, Thin Solid Films 518 (2010) 5463–5466. https://doi.org/10.1016/j.tsf.2010.04.018.
[134] H. Chatham, Oxygen diffusion barrier properties of transparent oxide coatings on polymeric substrates, Surf. Coating. Technol. 78 (1996) 1–9. https://doi.org/10.1016/0257-8972(95)02420-4.
[135] G. Rossi, M. Nulman, Effect of local flaws in polymeric permeation reducing barriers, J. Appl. Phys. 74 (1993) 5471–5475, https://doi.org/10.1063/1.354227.
[136] S.F. Lim, L. Ke, W. Wang, S.J. Chua, Correlation between dark spot growth and pinhole size in organic light-emitting diodes, Appl. Phys. Lett. 78 (2001) 2116–2118, https://doi.org/10.1063/1.1364658.
[137] V. Uwe, K. Daniel, R. Bernd, B. Gerd, R. Sven, H. Rigo, S. Michael, T. Michael, G. Christiane, A. Jörg, G. Sven-Thomas, P. Sebastian, H. Michael, V. Boris, Bidirectional OLED microdisplay for interactive see-through HMDs: study toward integration of eye-tracking and informational facilities, J. Soc. Inf. Disp. 17 (2009) 175–184, https://doi.org/10.1889/JSID17.3.175.
[138] J.D. Affinito, G.L. Graft, N. Greenwell, P.M. Martin, A new method for fabricating transparent barrier layers, Thin Solid Films 290–291 (1996) 63–67.
[139] J.D. Affinito, S. Eufinger, M.E. Gross, G.L. Graff, P.M. Martin, PML/oxide/PML barrier layer performance differences arising from use of UV or electron beam polymerization of the, PML layers 309 (1997) 19–25.
[140] P. Mandlik, L. Han, S. Wagner, J.A. Silvernail, R. Ma, M. Hack, J.J. Brown, P. Mandlik, L. Han, S. Wagner, J.A. Silvernail, R. Ma, Diffusion of atmospheric gases into barrier-layer sealed organic light emitting diodes Diffusion of atmospheric gases into barrier-layer sealed organic light, Appl. Phys. Lett. 93 (2008) 203306, https://doi.org/10.1063/1.3030982.
[141] G.S. Selwyn, Plasma particulate contamination control. I. Transport and process effects, J. Vac. Sci. Technol. B Microelectron. Nanometer Struct. Process. Meas. Phenom. 9 (1991) 3487–3492, https://doi.org/10.1116/1.585829.
[142] P.S. E, P.H. B, R. Robin, K.W.M. M, Room-temperature ALD of metal oxide thin films by energy-enhanced ALD, Chem. Vap. Depos. 19 (2013) 125–133, https://doi.org/10.1002/cvde.201207033.
[143] F.J. van den Bruele, M. Smets, A. Illiberi, Y. Creyghton, P. Buskens, F. Roozeboom, P. Poodt, Atmospheric pressure plasma enhanced spatial ALD of silver, J. Vac. Sci. Technol. A Vac. Surf. Film 33 (2015) 01A131, https://doi.org/10.1116/1.4902561.
[144] P.F. Carcia, R.S. McLean, M.D. Groner, A.A. Dameron, S.M. George, Gas diffusion ultrabarriers on polymer substrates using Al2O3 atomic layer deposition and SiN plasma-enhanced chemical vapor deposition, J. Appl. Phys. 106 (2009) 23533, https://doi.org/10.1063/1.3159639.
[145] S.-H.K. Park, J. Oh, C.-S. Hwang, J.-I. Lee, Y.S. Yang, H.Y. Chu, Ultrathin film encapsulation of an OLED by ALD, Electrochem. Solid State Lett. 8 (2005) H21, https://doi.org/10.1149/1.1850396.
[146] P.F. Carcia, R.S. McLean, M.H. Reilly, M.D. Groner, S.M. George, Ca test of Al2O3 gas diffusion barriers grown by atomic layer deposition on polymers, Appl. Phys. Lett. 89 (2006) 31915, https://doi.org/10.1063/1.2221912.
[147] T. Maindron, B. Aventurier, A. Ghazouani, T. Jullien, N. Rochat, J.-Y. Simon, E. Viasnoff, Investigation of Al2O3 barrier film properties made by atomic layer deposition onto fluorescent tris-(8-hydroxyquinoline) aluminium molecular films, Thin Solid Films 548 (2013) 517–525. https://doi.org/10.1016/j.tsf.2013.08.092.
[148] A.A. Dameron, S.D. Davidson, B.B. Burton, P.F. Carcia, R.S. McLean, S.M. George, Gas diffusion barriers on polymers using multilayers fabricated by Al2O3 and rapid SiO2 atomic layer deposition, J. Phys. Chem. C 112 (2008) 4573–4580, https://doi.org/10.1021/jp076866+.
[149] Y. Leterrier, Durability of nanosized oxygen-barrier coatings on polymers, Prog. Mater. Sci. 48 (2003) 1–55. https://doi.org/10.1016/S0079-6425(02)00002-6.
[150] L. Hoffmann, D. Theirich, S. Pack, F. Kocak, D. Schlamm, T. Hasselmann, H. Fahl, A. Räupke, H. Gargouri, T. Riedl, Gas diffusion barriers prepared by spatial atmospheric pressure plasma enhanced ALD, ACS Appl. Mater. Interfaces 9 (2017) 4171–4176, https://doi.org/10.1021/acsami.6b13380.
[151] M. Aghaee, P.S. Maydannik, P. Johansson, J. Kuusipalo, M. Creatore, T. Homola, D.C. Cameron, Low temperature temporal and spatial atomic layer deposition of TiO2 films, J. Vac. Sci. Technol. A Vac. Surf. Film 33 (2015) 041512, https://doi.org/10.1116/1.4922588.
[152] Y. Han, S. Meyer, Y. Dkhissi, K. Weber, J.M. Pringle, U. Bach, L. Spiccia, Y.-B. Cheng, Degradation observations of encapsulated planar CH3NH3PbI3 perovskite solar cells at high temperatures and humidity, J. Mater. Chem. A. 3 (2015) 8139–8147, https://doi.org/10.1039/C5TA00358J.
[153] B. Karim, M. Tony, K. Hani, Thin-film encapsulated white organic light top-emitting diodes using a WO3/Ag/WO3 cathode to enhance light out-coupling, J. Soc. Inf. Disp. 24 (2016) 563–568, https://doi.org/10.1002/jsid.466.
[154] B. Andreas, F. Christian, G. Tobias, T. Sara, B. Tim, Z. Kirill, P. Andreas, G. Patrick, R. Thomas, Highly robust transparent and conductive gas diffusion barriers based on tin oxide, Adv. Mater. 27 (2015) 5961–5967, https://doi.org/10.1002/adma.201502973.
[155] A. Bulusu, H. Kim, D. Samet, J.S. Graham, Improving the stability of atomic layer deposited alumina films in aqueous environments with metal oxide capping layers, J. Phys. D Appl. Phys. 46 (2013) 84014. http://stacks.iop.org/0022-3727/46/i=8/a=084014.
[156] B. Lee, R.V. Anderson, S.M. George, Metalcone and metalcone/metal oxide alloys grown using atomic & molecular layer deposition, Electrochem. Solid State Lett. Trans. 41 (2011) 131, https://doi.org/10.1149/1.3633661.
[157] P. Jin-Seong, C. Heeyeop, C. Ho Kyoon, L. Sang, In, Thin film encapsulation for flexible AM-OLED: a review, Semicond. Sci. Technol. 26 (2011) 34001. http://stacks.iop.org/0268-1242/26/i=3/a=034001.
[158] M. Park, S. Oh, H. Kim, D. Jung, D. Choi, J.-S. Park, Gas diffusion barrier characteristics of Al2O3/alucone films formed using trimethylaluminum, water and ethylene glycol for organic light emitting diode encapsulation, Thin Solid Films 546 (2013) 153–156. https://doi.org/10.1016/j.tsf.2013.05.017.
[159] D. Muñoz-Rojas, V.H. Nguyen, C. Masse de la Huerta, S. Aghazadehchors, C. Jiménez, D. Bellet, Spatial Atomic Layer Deposition (SALD), an emerging tool for energy materials. Application to new-generation photovoltaic devices and transparent conductive materials, Compt. Rendus Phys. 1 (2017) 1–10, https://doi.org/10.1016/j.crhy.2017.09.004.
[160] A. Illiberi, F. Roozeboom, P. Poodt, Spatial atomic layer deposition of zinc oxide thin films, ACS Appl. Mater. Interfaces 4 (2012) 268–272, https://doi.org/10.1021/am2013097.
[161] A. Illiberi, R. Scherpenborg, P. Poodt, F. Roozeboom, (Invited) spatial atomic layer deposition of transparent conductive oxides, ECS Trans. 58 (2013) 105–110, https://doi.org/10.1149/05810.0105ecst.
[162] A. Illiberi, T. Grehl, A. Sharma, B. Cobb, G. Gelinck, P. Poodt, H. Brongersma, F. Roozeboom, Spatial-ald of transparent and conductive oxides, meet, 2013, p. 1872. Abstr. MA2013-02, http://ma.ecsdl.org/content/MA2013-02/24/1872.abstract. (Accessed 6 February 2014).
[163] A. Illiberi, F. Grob, C. Frijters, P. Poodt, R. Ramachandra, H. Winands, M. Simor, P.J. Bolt, High rate (~7 nm/s), atmospheric pressure deposition of ZnO front electrode for Cu(In,Ga)Se 2 thin-film solar cells with efficiency beyond 15%, Prog. Photovoltaics Res. Appl. 21 (2013) 1559–1566, https://doi.org/10.1002/pip.2423.
[164] a. Illiberi, R. Scherpenborg, F. Roozeboom, P. Poodt, Atmospheric spatial atomic layer deposition of in-doped ZnO, ECS J. Solid State Sci. Technol. 3 (2014) P111–P114, https://doi.org/10.1149/2.002405jss.
[165] A. Illiberi, B. Cobb, A. Sharma, T. Grehl, H. Brongersma, F. Roozeboom, G. Gelinck, P. Poodt, Spatial atmospheric atomic layer deposition of InxGayZnzO for thin films, ACS Appl. Mater. Interfaces (2015), https://doi.org/10.1021/am508071y, 150204105923009.
[166] V.H. Nguyen, J. Resende, C. Jiménez, J.-L. Deschanvres, P. Carroy, D. Muñoz, D. Bellet, D. Muñoz-Rojas, Deposition of ZnO based thin films by atmospheric pressure spatial atomic layer deposition for application in solar cells, J. Renew. Sustain. Energy 9 (2017) 021203, https://doi.org/10.1063/1.4979822.
[167] C.H. Frijters, P. Poodt, A. Illiberi, Atmospheric spatial atomic layer deposition of Zn(O,S) buffer layer for Cu(In,Ga)Se2 solar cells, Sol. Energy Mater. Sol. Cells 155 (2016) 356–361, https://doi.org/10.1016/j.solmat.2016.06.016.
[168] R.L.Z. Hoye, K.P. Musselman, M.R. Chua, A. Sadhanala, R.D. Raninga, R.H. Friend, D. Credgington, Bright and efficient blue polymer light emitting, J. Mater. Chem. C. 3 (2015) 9327–9336, https://doi.org/10.1039/C5TC01581B.
[169] A. Illiberi, I. Katsouras, S. Gazibegovic, B. Cobb, E. Nekovic, W. Van Boekel, C. Frijters, J. Maas, F. Roozeboom, Y. Creyghton, P. Poodt, G. Gelinck, Atmospheric plasma-enhanced spatial-ALD of InZnO for high mobility thin film transistors, J. Vac. Sci. Technol. A Vac. Surfaces Film 36 (2018) 2–9, https://doi.org/10.1116/1.5008464.
[170] P. Poodt, B. Kniknie, A. Branca, H. Winands, F. Roozeboom, Patterned deposition by plasma enhanced spatial atomic layer deposition, Phys. Status Solidi Rapid Res. Lett. 5 (2011) 165–167, https://doi.org/10.1002/pssr.201004542.
[171] Y. Creyghton, A. Illiberi, A. Mione, W. van Boekel, N. Debernardi, M. Seitz, F. van den Bruele, P. Poodt, F. Roozeboom, Plasma-enhanced atmospheric-pressure spatial ALD of Al 2 O 3 and ZrO 2 Y. Creyghton, ECS Trans. 75 (2016) 11–19.
[172] T. Faraz, H.C.M. Knoops, M.A. Verheijen, C.A.A. van Helvoirt, S. Karwal, A. Sharma, V. Beladiya, A. Szeghalmi, D.M. Hausmann, J. Henri, M. Creatore, W.M.M. Kessels, Tuning material properties of oxides and nitrides by substrate biasing during plasma-enhanced atomic layer deposition on planar and 3D substrate topographies, ACS Appl. Mater. Interfaces 10 (2018) 13158–13180, https://doi.org/10.1021/acsami.8b00183.
[173] R. Chen, H. Kim, P.C. McIntyre, D.W. Porter, S.F. Bent, Achieving area-selective atomic layer deposition on patterned substrates by selective surface modification, Appl. Phys. Lett. 86 (2005) 1–3, https://doi.org/10.1063/1.1922076.
[174] R. Chen, S.F. Bent, Chemistry for positive pattern transfer using area-selective atomic layer deposition, Adv. Mater. 18 (2006) 1086–1090, https://doi.org/10.1002/adma.200502470.

[175] X. Jiang, S.F. Bent, Area-selective ALD with soft lithographic methods: using self-assembled monolayers to direct film deposition, J. Phys. Chem. C 113 (2009) 17613–17625, https://doi.org/10.1021/jp905317n.
[176] A. Mameli, Y. Kuang, M. Aghaee, C.K. Ande, B. Karasulu, M. Creatore, A.J.M. Mackus, W.M.M. Kessels, F. Roozeboom, Area-selective atomic layer deposition of In2O3:H using a μ-plasma printer for local area activation, Chem. Mater. 29 (2017) 921–925, https://doi.org/10.1021/acs.chemmater.6b04469.
[177] K.J. Kanarik, T. Lill, E.A. Hudson, S. Sriraman, S. Tan, J. Marks, V. Vahedi, R.A. Gottscho, Overview of atomic layer etching in the semiconductor industry, J. Vac. Sci. Technol. A Vac. Surf. Film 33 (2015) 020802, https://doi.org/10.1116/1.4913379.
[178] F. Roozeboom, F. van den Bruele, Y. Creyghton, P. Poodt, W.M.M. Kessels, Cyclic etch/passivation-deposition as an all-spatial concept toward high-rate room temperature atomic layer etching, ECS J. Solid State Sci. Technol. 4 (2015) N5067–N5076, https://doi.org/10.1149/2.0111506jss.